



# Design, green synthesis, molecular docking and anticancer evaluations of diazepam bearing sulfonamide moieties as VEGFR-2 inhibitors

Nashwa M. Saleh<sup>a,\*</sup>, Mohamed S.A. El-Gaby<sup>b</sup>, Khaled El-Adl<sup>c,d,\*</sup>, Nour E.A. Abd El-Sattar<sup>e</sup>

<sup>a</sup> Department of Chemistry, Faculty of Science, Al-Azhar University (Girls Branch), PO Box 11754, Cairo, Egypt

<sup>b</sup> Department of Chemistry, Faculty of Science, Al-Azhar University at Assiut, Assiut 71524, Egypt

<sup>c</sup> Pharmaceutical Medicinal Chemistry and Drug Design Department, Faculty of Pharmacy (Boys), Al-Azhar University, Nasr City 11884, Cairo, Egypt

<sup>d</sup> Pharmaceutical Chemistry Department, Faculty of Pharmacy, Heliopolis University for Sustainable Development, Cairo, Egypt

<sup>e</sup> Department of Chemistry, Faculty of Science, Ain Shams University, Cairo, Egypt

## ARTICLE INFO

### Keywords:

Benzodiazepines  
Sulfonamide  
Molecular docking  
VEGFR-2 inhibitors  
Anticancer agents

## ABSTRACT

Novel series of diazepam bearing sulfonamide moieties **5<sub>a-f</sub>** and **7<sub>a-c</sub>** were designed, synthesized and evaluated for anticancer activity against HepG2, HCT-116 and MCF-7 cell lines. MCF-7 was the most sensitive cell line to the influence of the new derivatives. In particular, compound **5<sub>d</sub>** was found to be the most potent derivative overall the tested compounds against the three HepG2, HCT116 and MCF-7 cancer cell lines with  $IC_{50} = 8.98 \pm 0.1$ ,  $7.77 \pm 0.1$  and  $6.99 \pm 0.1 \mu\text{M}$  respectively. Compound **5<sub>d</sub>** exhibited higher activity than sorafenib, ( $IC_{50} = 9.18 \pm 0.6$ ,  $5.47 \pm 0.3$  and  $7.26 \pm 0.3 \mu\text{M}$  respectively), against HepG2 and MCF-7 but exhibited lower activity against HCT116 cancer cell lines respectively. Also, this compound displayed lower activity than doxorubicin, ( $IC_{50} = 7.94 \pm 0.6$ ,  $8.07 \pm 0.8$  and  $6.75 \pm 0.4 \mu\text{M}$  respectively), against HepG2 and MCF-7 but higher activity against HCT116 cell lines respectively. Compounds **5<sub>b</sub>**, **5<sub>c</sub>**, **5<sub>d</sub>**, **5<sub>e</sub>**, **5<sub>f</sub>** and **7<sub>c</sub>** are respectively, 5.77, 8.58, 9.54, 5.71, 4.68 and 2.31 fold times more toxic in breast cancer cell lines (MCF-7, the most sensitive cells) than in VERO normal cells. All the synthesized compounds **5<sub>a-f</sub>** and **7<sub>a-c</sub>** were evaluated for their inhibitory activities against VEGFR-2. Among them, compound **5<sub>d</sub>** was found to be the most potent derivative that inhibited VEGFR-2 at  $IC_{50}$  value of  $0.10 \pm 0.01 \mu\text{M}$ , which is equipotent to sorafenib  $IC_{50}$  value ( $0.10 \pm 0.02 \mu\text{M}$ ). Compound **5<sub>e</sub>** exhibited excellent activity with  $IC_{50}$  value of  $0.12 \pm 0.01 \mu\text{M}$  which nearly equipotent to that of sorafenib. Compounds **5<sub>b</sub>**, **5<sub>c</sub>** and **5<sub>f</sub>** exhibited very good activity with the same  $IC_{50}$  value of  $0.14 \pm 0.02 \mu\text{M}$ . Also, compounds **7<sub>c</sub>** and **7<sub>b</sub>** possessed good VEGFR-2 inhibition with  $IC_{50}$  values of  $0.16 \pm 0.06$  and  $0.17 \pm 0.06 \mu\text{M}$  respectively which are more than the half activity of that of sorafenib. The data obtained from docking studies were highly correlated with that obtained from the biological screening.

## 1. Introduction

Green and sustainable chemistry refers to the design of chemical products and processes that reduce or eliminate the use and formation of hazardous chemicals. Therefore, green chemistry practices are intended to provide economic and environmental benefits to society as a whole [1]. Chemists can greatly reduce risks to both human health and the environment by reducing or eliminating hazardous substances usage or generation associated with a particular synthesis or process.

In this work, all reactions were carried out at room temperature to decrease energy usage so increasing energy efficiency. Also, it focused in designing less hazardous chemical syntheses, designing safer chemicals

and products. Moreover, using the preferred safer solvents such as ethanol and/or acetone and safer reaction conditions (room temperature).

Benzodiazepines (BDZ's) are privileged bicyclic heteroaromatic compounds and were considered as an essential class of pharmacologically active analogues in medicinal and pharmaceutical chemistry [2–6]. Benzodiazepines are primarily known for their depression in the central nervous system [7]. In addition to their established anxiolytic activities, 1,4-benzodiazepines and their analogues demonstrated diversity of activity such as antimicrobial [8], in alcohol withdrawal syndrome [9], sedative [10], hypnotic [11,12], anxiolytic [10,13], anticonvulsant [14], analgesic [15], anti-inflammatory [16], anti-

\* Corresponding authors at: Pharmaceutical Medicinal Chemistry and Drug Design Department, Faculty of Pharmacy (Boys), Al-Azhar University, Nasr City 11884, Cairo, Egypt (K. El-Adl).

E-mail addresses: [dmashwamostafa@azhar.edu.eg](mailto:dmashwamostafa@azhar.edu.eg) (N.M. Saleh), [eladlkhale74@yahoo.com](mailto:eladlkhale74@yahoo.com), [eladlkhale74@azhar.edu.eg](mailto:eladlkhale74@azhar.edu.eg), [khaled.eladl@hu.edu.eg](mailto:khaled.eladl@hu.edu.eg) (K. El-Adl).

<https://doi.org/10.1016/j.bioorg.2020.104350>

Received 19 July 2020; Received in revised form 10 September 2020; Accepted 3 October 2020

Available online 8 October 2020

0045-2068/© 2020 Elsevier Inc. All rights reserved.

platelet anti-ulcer [17], antipsychotics [18], anti-proliferative [19] and anticancer activities [2,7,20–22]. Diazepam consistently inhibited Fatty acid synthase (FAS) activity, a known anticancer mechanism of flavonoids, in addition, it inhibited the release of vascular endothelial growth factor (VEGF) [23].

Sulfonamide moieties attached to different heterocyclic compounds have been reported to inhibit the growth of human tumor cell lines [24–28]. Ghorab et al. [29] designed (quinoxalin-2-yl)benzene sulfonamide derivative I (Fig. 1) with a potent anti-cancer activity against human liver cancer cell line (Hep G2). In 2014, Shahin et al. [30] designed a series of new sulfonamide moieties joined to quinoxaline scaffolds which were biologically evaluated for their inhibitory activity against VEGFR-2. Also, compound II (Fig. 1) displayed very good anticancer activities against HepG2, HCT-116 and MCF-7 cell lines with  $IC_{50}$  values of 24.5, 12 and 10.23  $\mu$ M respectively, while compound III (Fig. 1) exhibited  $IC_{50}$  values of 22.9, 21.9 and 22.9  $\mu$ M respectively [31].

Owing to the promising biological activities of benzodiazepines and sulfonamide derivatives we aimed at incorporation of sulfonamide moieties into diazepam which may act as potential anticancer molecules targeting VEGFR-2 enzyme.

Human protein tyrosine kinases (PTKs) play a fundamental role in human carcinogenesis [32], whereas a cascade of protein kinases controlled cell cycle progression, cell division and proliferation as a sequence of events, so PTKs have emerged as promising new cancer therapy targets [33].

The vascular endothelial growth factor (VEGF) is a positive regulator with its distinct specificity for vascular endothelial cells. The biological action of VEGF is mediated by three structurally related receptors, VEGFR-1 (Flt-1), VEGFR-2 (KDR/Flk-1) and VEGFR-3 [34]. VEGFR-2, a

tyrosine kinase subtype, is the major regulator of VEGF-driven responses in endothelial cells and can mediate proliferation, differentiation, and microvascular permeability. Moreover, it has proven to be a prerequisite signal transducer in both physiologic and pathologic angiogenesis [35,36]. VEGFR-2 is over-expressed in several malignancies, including hepatocellular carcinoma, breast, colorectal, ovarian and thyroid cancer, melanoma and medulloblastoma [37–39]. Therefore, VEGFR-2 has been identified as an excellent remedial target for the production of novel anticancer agents [40]. Hence, inhibition of VEGFR-2 pathway has attracted widespread interest as an approach to anti-cancer therapy [41]. In addition, inhibition of VEGF signaling can also change or destroy tumor vessels. VEGFR-2 inhibitors, as TKIs, prevent the vital processes of angiogenesis and lymph angiogenesis. Recently, it was reported that a number of compounds have been confirmed as potent inhibitors of VEGFR-2 in vitro or possessed antiangiogenic activity and achieved clinical success in the treatment of cancer [42]. Due to the important role of VEGFR-2 in angiogenesis, this receptor is the most vital target in anti-angiogenic therapy against cancer. Several potent VEGFR-2 inhibitors have been developed and approved for treatment of various cancers, e.g. Pazopanib (IV) [20,43], sunitinib (V) [44,45] and Sorafenib (Nexavar)<sup>®</sup>(VI) [46–48] (Fig. 1).

In continuation of our previous efforts in the field of design and synthesis of new anticancer agents, especially VEGFR-2 inhibitors [49–56], a new series of diazepam bearing sulfonamide moieties were designed and synthesized on the basis of the main pharmacophoric features of VEGFR-2 inhibitors.

A study of the structure–activity relationships (SAR) and binding pattern of sorafenib and various VEGFR-2 inhibitors revealed that they shared four main features (as shown in Fig. 2) [57–61]; (i) A flat hetero aromatic ring system. (ii) A central aryl ring (hydrophobic spacer). (iii)

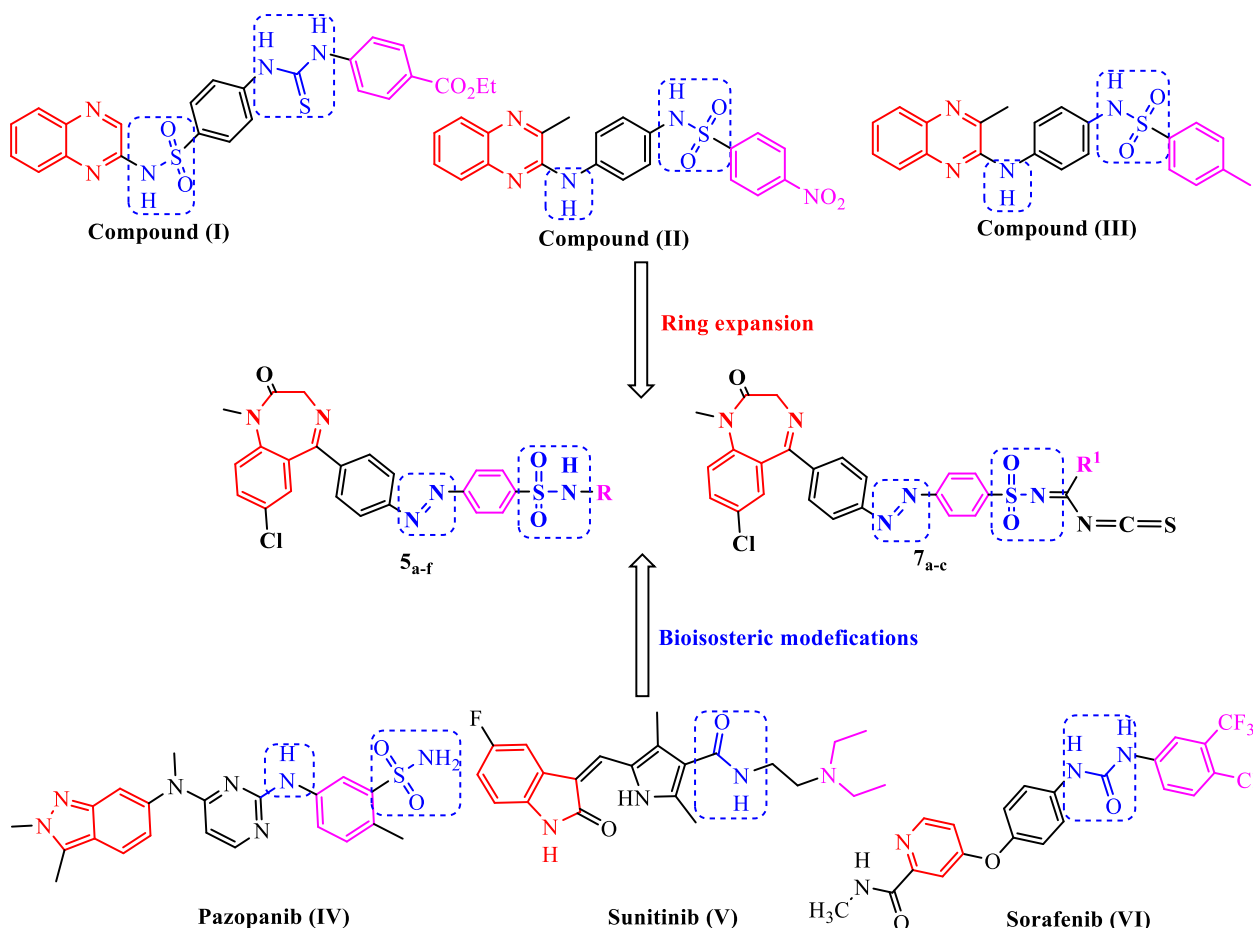


Fig. 1. Reported VEGFR-2 inhibitors and our derivatives.

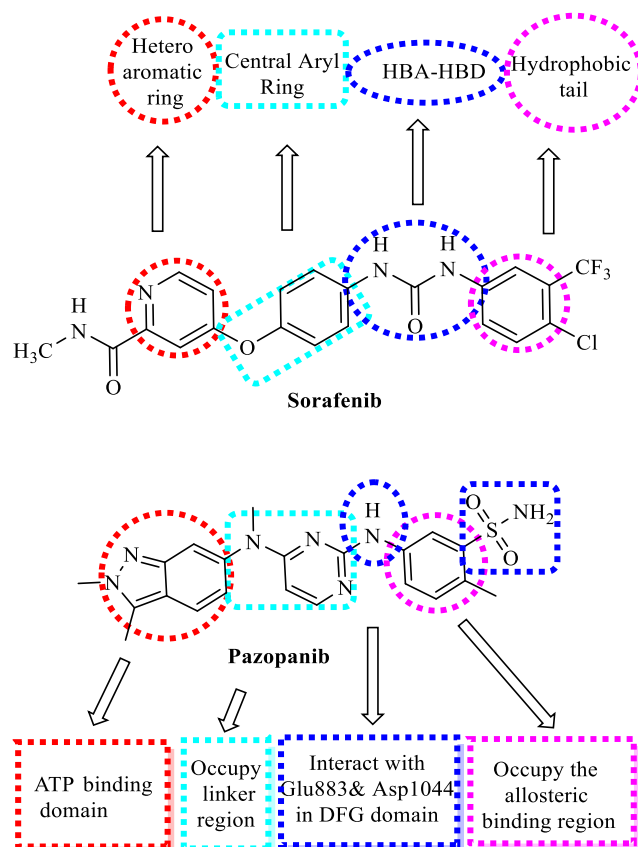


Fig. 2. The basic structural requirements for sorafenib and pazopanib as reported VEGFR-2 inhibitors.

A linker containing a functional group acting as pharmacophore (e.g. amino or urea) that possesses both H-bond acceptor (HBA) and donor (HBD) in order to bind with two crucial residues (Glu883 and Asp1044). (iv) The terminal hydrophobic moiety that occupies the newly created allosteric hydrophobic pocket *via* various hydrophobic interactions.

The goal of our work is to synthesize new diazepam bearing sulfonamide moieties with the same essential pharmacophoric features of the reported and clinically used VEGFR-2 inhibitors, in addition, to being molecularly hybridized in an attempt to get more potent anti-tumor molecules. The main core of our molecular design rationale was carried out by ring expansion and bioisosteric modification strategies of VEGFR-2 inhibitors (sorafenib & pazopanib) at four different positions (Fig. 3).

In general, the designed compounds were synthesized and evaluated for their *in vitro* anti-proliferative activities against three human tumor cell lines, namely, hepatocellular carcinoma (HCC) type (HepG2), breast cancer (Michigan Cancer Foundation-7 (MCF-7)) and human colorectal carcinoma-116 (HCT-116). The results prompted further examinations to reach a deep insight into the mechanism of action of the synthesized compounds. Molecular docking studies were conducted to understand the expected binding interactions of the target compounds with VEGFR-2 active sites. Moreover, the most active cytotoxic compounds that showed promising  $IC_{50}$  values against the three cancer cell lines were subjected to further investigation for their tyrosine kinase inhibitory activities against VEGFR-2.

### 1.1. Rationale and structure-based design

Diazepam bearing sulfonamide derivatives have the essential pharmacophoric features of VEGFR-2 inhibitors (Fig. 3) which include: the presence of seven membered hetero ring diazepine, fused with benzene

ring (as hydrophobic group), to replace the pyridine and 2,3-dimethyl-2H-indazole moieties of the reference ligands sorafenib and pazopanib, respectively. Moreover, phenyldiazene spacer was designed to replace the central aryl and the methylaminopyrimidine rings of the reference ligands sorafenib and pazopanib, respectively. Furthermore, the benzodiazepine moiety occupied the hydrophobic groove formed by *Leucine1033*, *Glycine920*, *Lysine918*, *Cysteine917*, *Phenylalanine916*, *Glutamate915*, *Alanine864* and *Leucine838* (Fig. 4).

The diazene and/or sulfonamide linkers interact as H-bond acceptor and as H-bond donor through N=N and NH respectively forming H-bonds with the essential amino acid residues *Aspartate1044*. Also the terminal (un)substituted hydrophobic tails occupied the hydrophobic pocket formed by *Aspartate1044*, *Cysteine1043*, *Isoleucine1042*, *Valine897*, *Leucine887*, *Lysine866* and *Glutamate883*. Moreover, the distal hydrophobic moieties attached to sulfonamide linkers in order to increase the length of the structure to enable these distal moieties to occupy new hydrophobic grooves formed by *Arginine1025*, *Histidine1024*, *Isoleucine1023*, *Cysteine1022*, *Lysine1021*, *Arginine1020*, *Leucine1017*, *Isoleucine890*, *Histidine889* and *Isoleucine886* (Fig. 4).

## 2. Results and discussion

### 2.1. Chemistry

At first, the authors expected to get the addition of diazonium salt at position-3 of diazepam according to the reported procedures [62,63] and/or at *ortho*-position of the 5-phenyl ring [64–66] so will obtain mixture of the corresponding derivatives 3 and/or 4 respectively (Fig. 5).

But the provided data ensure the addition was occurred at the preferred *para*-position (substitution of the activated aromatic ring by the electrophilic aryldiazonium ion occurs principally at the *para* position. However, if the *para* position is blocked by a substituent, substitution occurs at the *ortho* position) [66] due to low temperature, electronic and steric effects (Fig. 6) and resulted in the corresponding pure 5<sub>a-f</sub> derivatives respectively (Scheme 1).

The possible reaction mechanism is proposed as described at Fig. 6, through an electrophilic aromatic substitution. Initially, the acetate anion catalyst activates the methylene group in the diazepam 2 through the abstract of a proton to yield the non-isolable intermediate (A) (this mechanism is very similar to aldol condensation where a carbanion is generated [67]) which is then stabilized by resonance and delocalization of the negative charge due to the group the aromatic ring. Finally, the intermediate (A) then undergo coupling with the beta-nitrogen of a diazonium ion and subsequent proton transfer to yield the final product 5. The preferred *para* attack occurs in the reaction of diazepam 2 with diazonium cation was attributed to the steric effect that inhibited at the *ortho*-position [66].

The formation of 7<sub>a-c</sub> is assumed to proceed through nucleophilic attack of the amino functional group of compound 5<sub>a</sub> to the thiocarbonyl moiety of isothiocyanate followed by intramolecular cyclization *via* the addition of NH to carbonyl group to form the non-isolable intermediate (B) (1,3-diazetidene). The latter intermediate (B) then undergoes a further stabilization *via* an intramolecular rearrangement [68] under the reaction conditions by removal of water molecule to give the unsaturated isothiocyanate 7<sub>a-c</sub> (Fig. 7).

The synthetic strategy for preparation of the target compounds (5<sub>a-f</sub> 7<sub>a-c</sub>) is depicted in Schemes 1 and 2. Synthesis was initiated by addition of sodium nitrite solution to acidic solution of 4-aminobenzenesulfonamide to obtain the corresponding diazonium salt solution, following the reported procedure [69], which underwent reaction with diazepam 2 in ethanol in the presence of sodium acetate to obtain the corresponding derivatives 5<sub>a-f</sub> respectively (Scheme 1).

The infrared spectra of compounds 5<sub>a-f</sub> revealed carbonyl absorption band at 1685  $cm^{-1}$  typical of unsaturated lactams; also, absorption bands belonging to N=N at 1596–1603  $cm^{-1}$  and showed absorptions at

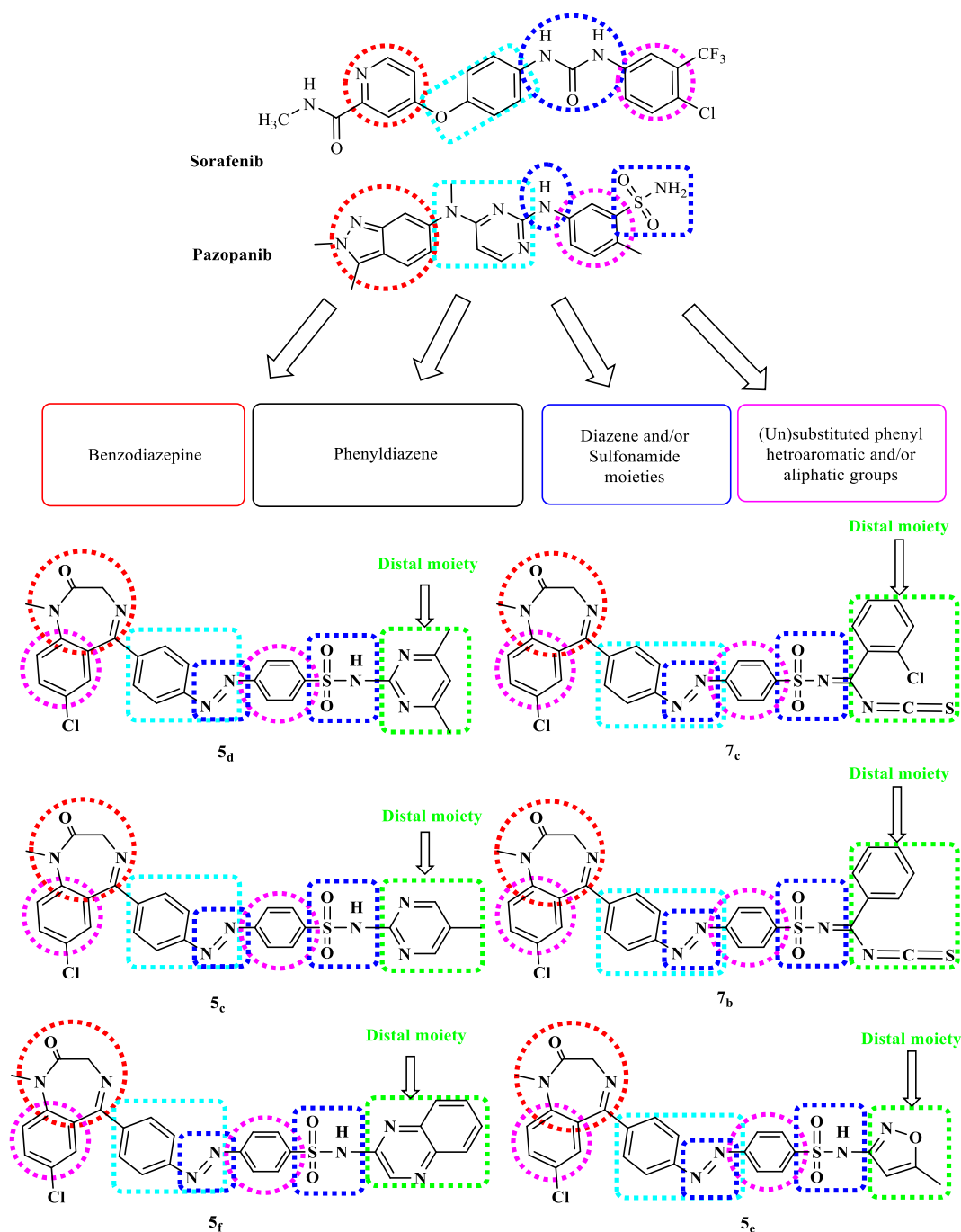


Fig. 3. Structural similarities and pharmacophoric features of VEGFR-2 inhibitors and some designed compounds.

3419–3444  $\text{cm}^{-1}$  for the NH group. In the  $^1\text{H}$  NMR spectra of 5<sub>a-f</sub> two doublets were observed at  $\delta$  3.80–3.92 and 4.60 ppm with the same coupling constant ( $J = 10.8$  Hz) assigned to the methylene protons on C-3 of diazepam ring, a singlet at  $\delta$  3.27–3.39 ppm as assigned to the methyl protons in addition to the presence of the aromatic protons. Furthermore, the  $^{13}\text{C}$  NMR spectra for these compounds displayed all the expected signals. The representative  $^{13}\text{C}$  NMR spectrum of compound 5<sub>b</sub> (DMSO- $d_6$ ) revealed the appearance of a signal at 168.96 due to the presence of C=O group and showed three signals at 168.38, 155.73 and 155.60 which were assigned to the three C=N as well as signals at  $\delta$  154.34, 152.70, 131.18, 130.99, 130.52, 129.84, 129.52, 122.83, 122.48, 121.51, 119.98 due to the aromatic carbons and signals at  $\delta$  55.91 ( $\text{CH}_2$ ) and 34.15 ( $\text{CH}_3$ ).

The chemistry of acyl isothiocyanates is very complex, varied and

used for synthesizing certain organic substances of biological significance [70]. Acyl isothiocyanates are bi-functional compounds which containing a carbonyl group and a thiocyanate group. They are highly reactive due to the presence of the flow of electrons-withdrawing acyl group. Thus, the reactivity of acyl isothiocyanates are, determined by three active centers; the electrophilic carbon atoms of the carbonyl and thiocarbonyl groups as well as the nucleophilic nitrogen atom, which enable them to participate in various types of addition and cyclization reactions. The behavior of benzene sulfonamide 5<sub>a</sub> towards acyl isothiocyanate was examined. Room temperature reaction of benzene sulfonamide derivative 5<sub>a</sub> with acetyl isothiocyanate in dry acetone gave the acetimidoyl isothiocyanate 7<sub>a</sub> in quantitative yield, rather than the expected acyl thioureas 6<sub>a</sub>. The infrared spectrum of the reaction product indicated the absence of the  $\text{NH}_2$  absorption bands and contains

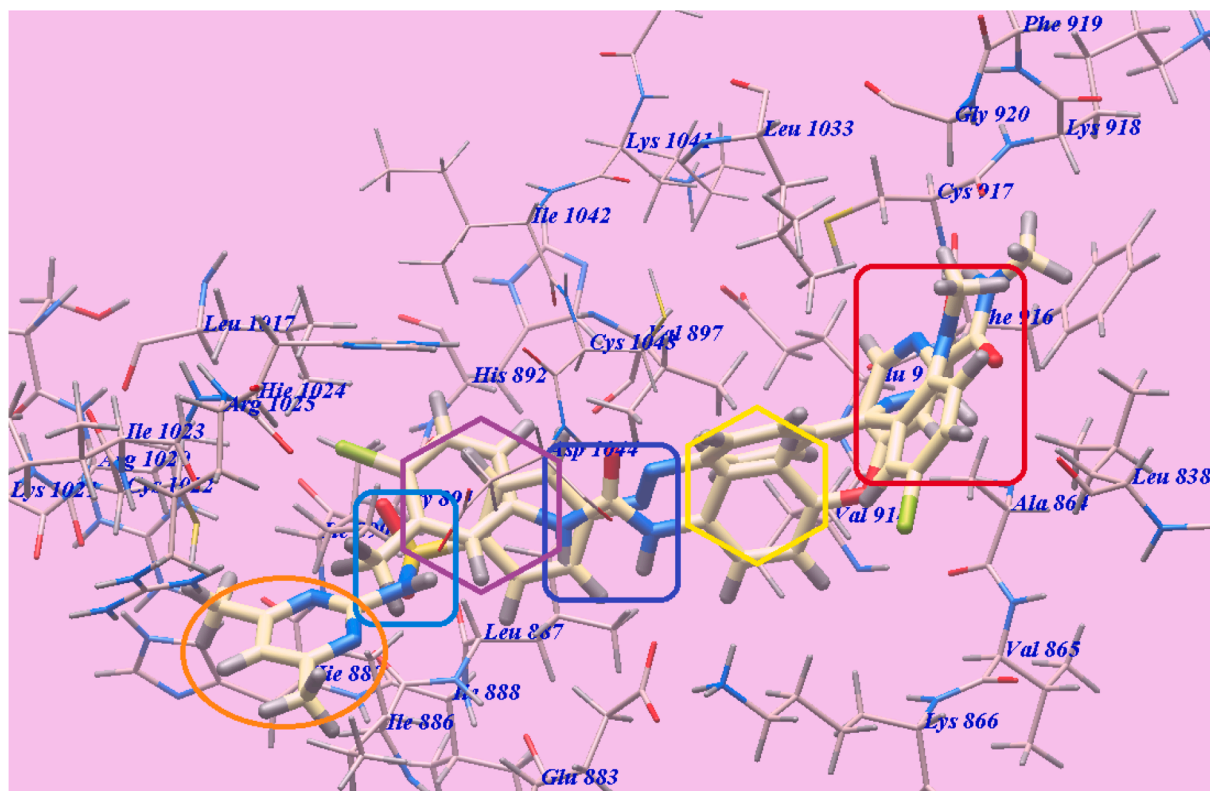


Fig. 4. Superimposition of compound **5<sub>d</sub>** and sorafenib inside the binding pocket of 1YWN.

the characteristic absorption band at  $2120\text{ cm}^{-1}$  was assigned for the  $\text{N}=\text{C}=\text{S}$  group and three absorption bands at  $1865$ ,  $1631$  and  $1601\text{ cm}^{-1}$  assignable for  $\text{C}=\text{O}$ ,  $\text{C}=\text{N}$  and  $\text{N}=\text{N}$  groups, respectively. The  $^1\text{H}$ NMR spectrum ( $\text{DMSO-}d_6$ ) of the reaction product showed absence of the singlet signal assignable for  $\text{NH}_2$  while revealed two doublets at  $\delta$  3.96 and 4.58 ppm with the same coupling constant ( $J = 10.8\text{ Hz}$ ) assigned to the methylene protons and two singlet signals at  $\delta$  2.09 and 3.35, ppm assigned to the two methyl protons in addition to the presence of the aromatic protons.

In a similar manner, treatment of benzene sulfonamide derivative **5<sub>a</sub>** with benzoylisothiocyanate and 2-chlorobenzoylisothiocyanate in acetone at room temperature yielded the corresponding benzimidoylisothiocyanate (**7<sub>b</sub>**) and 2-chlorobenzimidoylisothiocyanate (**7<sub>c</sub>**) derivatives respectively (Scheme 2).

The structures of (**7<sub>b,c</sub>**) were established on their respective analytical and spectral data. The infrared spectra of compounds **7<sub>b,c</sub>** showed the disappearance of absorption bands for  $\text{NH}_2$  and showed the appearance of absorption band for  $\text{C}=\text{O}$ ,  $\text{C}=\text{N}$  and  $\text{N}=\text{N}$  groups, while strong absorption band appeared at  $2130\text{ cm}^{-1}$  for  $\text{N}=\text{C}=\text{S}$  group. The  $^1\text{H}$ NMR spectra ( $\text{DMSO-}d_6$ ) of compounds (**7<sub>b,c</sub>**) showed two doublets at  $\delta$  3.81–3.98 and 4.57–4.60 ppm with the same coupling constant ( $J = 10.8\text{ Hz}$ ) which were assigned to the protons of methylene moiety in addition to the presence of sharp singlet at  $\delta$  3.34–3.35 ppm assigned to the methyl protons as well as aromatic protons. The  $^{13}\text{C}$  NMR spectrum of compound **7<sub>b</sub>** revealed the presence of a signal at  $143.0$  due to the presence of  $\text{N}=\text{C}=\text{S}$  group and signals at  $\delta$  35.25 ( $\text{CH}_3$ ), 56.2 ( $\text{CH}_2$ ), 151 ( $\text{C}=\text{N}$ ), 168 ( $\text{C}=\text{O}$ ) in addition to the presence of aromatic carbons.

## 2.2. Docking studies

All modeling experiments were carried out using Molsoft software. Each experiment used VEGFR-2 downloaded from the Brookhaven Protein Databank (PDB ID 1YWN) [71].

The obtained results indicated that all studied ligands have similar

position and orientation inside the recognized binding site of VEGFR-2 that reveals a large space bounded by a membrane-binding domain, which serves as entry channel for substrate to the active site (Fig. 8). The obtained results of the free energy of binding ( $\Delta G$ ) explained that most of these compounds had good binding affinity toward the receptor and the computed values reflected the overall trend (Table 1).

The proposed binding mode of **sorafenib** revealed affinity value of  $-95.66\text{ kcal/mol}$  and 4 H-bonds. The urea linker formed one H-bond with the key amino acid *Glutamate883* ( $2.13\text{ \AA}$ ) through its NH group and one H-bond with *Aspartate1044* ( $1.53\text{ \AA}$ ) through its carbonyl group. The *N*-methylpicolinamide moiety was stabilized by formation of 2 H-bonds with *Cysteine917* where, the pyridine N atom formed 1H-bond with the NH of *Cysteine917* ( $2.46\text{ \AA}$ ) while its NH group formed 1H-bond with the carbonyl of *Cysteine917* ( $2.20\text{ \AA}$ ). The *N*-methylpicolinamide moiety occupied the hydrophobic groove formed by *Leucine1033*, *Glycine920*, *Lysine918*, *Cysteine917*, *Phenylalanine916*, *Glutamate915*, *Leucine838* and *Alanine864*. Moreover, the central phenyl ring occupied the hydrophobic pocket formed by *Cysteine1043*, *Leucine1033*, *Valine914*, *Valine897* and *Lysine866*. Furthermore, the hydrophobic 3-trifluoromethyl-4-chlorophenyl moiety attached to the urea linker occupied the hydrophobic pocket formed by *Aspartate1044*, *Isoleucine1042*, *Histidine1024*, *Leucine1017*, *Isoleucine890* and *Leucine887* (Fig. 9). The urea linker played an important role in the binding affinity towards VEGFR-2 enzyme, where it was responsible for the higher binding affinity of **sorafenib**. These findings encourage us to use diazene and sulfonamide linkers hoping to obtain potent VEGFR-2 inhibitors.

The proposed binding mode of compound **5<sub>d</sub>** is virtually the same as that of **sorafenib** which revealed higher affinity value of  $-116.78\text{ kcal/mol}$  and 5H-bonds. The carbonyl group of diazepame scaffold formed one H-bond with the essential amino acid *Cysteine917* through its NH group with a distance of  $1.93\text{ \AA}$ . Moreover, the diazene linker formed 2H-bonds with *Aspartate1044* ( $2.06\text{ \AA}$ ,  $2.79\text{ \AA}$ ) while NH group of sulfonamide moiety formed a third H bond with *Aspartate1044* ( $1.75\text{ \AA}$ ).

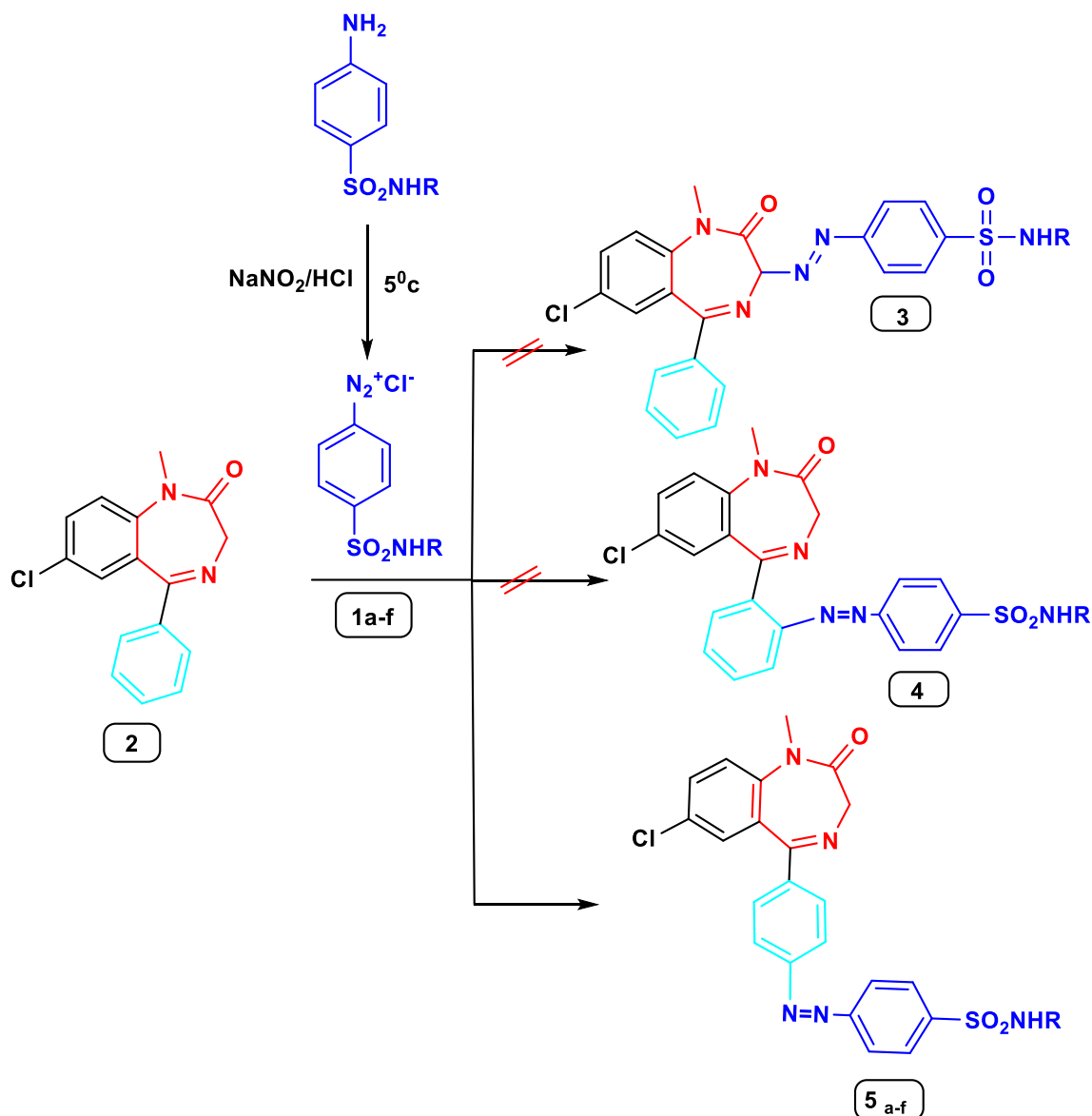


Fig. 5. Addition of the diazonium salt at *para*-position of the phenyl ring at position-5 of diazepam.

Furthermore, the N atom of the distal pyridine moiety formed one H-bond with *Arginine1025* (2.95 Å). The diazepam scaffold occupied the hydrophobic groove formed by *Leucine1033*, *Glycine920*, *Lysine918*, *Cysteine917*, *Phenylalanine916*, *Glutamate915*, *Alanine864* and *Leucine838*. Moreover, the central phenyldiazene spacer occupied the hydrophobic pocket formed by *Aspartate1044*, *Cysteine1043*, *Leucine1033*, *Glutamate915*, *Valine914*, *Valine897* and *Lysine866*. The hydrophobic phenyl tail occupied the hydrophobic pocket formed by *Aspartate1044*, *Cysteine1043*, *Isoleucine1042*, *Valine897*, *Leucine887*, *Lysine866* and *Glutamate883*. Furthermore, the distal 4,6-dimethylpyridine moiety occupied the hydrophobic groove formed by *Arginine1025*, *Histidine1024*, *Isoleucine1023*, *Cysteine1022*, *Lysine1021*, *Arginine1020*, *Leucine1017*, *Isoleucine890*, *Histidine889* and *Isoleucine886* (Fig. 10). These interactions of compound 5<sub>d</sub> may explain its highest anticancer activity.

The proposed binding mode of compound 5<sub>c</sub> is virtually the same as that of *sorafenib* and 5<sub>d</sub> which revealed higher affinity value of -107.58 kcal/mol and 5H-bonds. The carbonyl group of diazepam scaffold formed one H-bond with the essential amino acid *Cysteine917* (1.91 Å). Moreover, the diazene linker formed 2H-bonds with *Aspartate1044* (2.27 Å, 2.47 Å) while NH group of sulfonamide moiety formed

a third H bond with *Aspartate1044* (2.17 Å). Furthermore, the N atom of the distal pyridine moiety formed one H-bond with *Arginine1025* (2.98 Å). The diazepam scaffold occupied the hydrophobic groove formed by *Leucine1033*, *Glycine920*, *Lysine918*, *Cysteine917*, *Phenylalanine916*, *Glutamate915*, *Alanine864* and *Leucine838*. Moreover, the central phenyldiazene spacer occupied the hydrophobic pocket formed by *Aspartate1044*, *Cysteine1043*, *Leucine1033*, *Glutamate915*, *Valine914*, *Valine897* and *Lysine866*. The hydrophobic phenyl tail occupied the hydrophobic pocket formed by *Aspartate1044*, *Cysteine1043*, *Isoleucine1042*, *Valine897*, *Leucine887*, *Lysine866* and *Glutamate883*. Furthermore, the distal 5-methylpyridine moiety occupied the hydrophobic groove formed by *Arginine1025*, *Histidine1024*, *Isoleucine1023*, *Cysteine1022*, *Lysine1021*, *Arginine1020*, *Leucine1017*, *Isoleucine890*, *Histidine889* and *Isoleucine886* (Fig. 11). These interactions of compound 5<sub>c</sub> may explain its high anticancer activity.

The proposed binding mode of compound 5<sub>f</sub> is virtually the same as that of *sorafenib* and 5<sub>d</sub> which revealed higher affinity value of -101.97 kcal/mol and 5H-bonds. The carbonyl group of diazepam scaffold formed one H-bond with the essential amino acid *Cysteine917* (1.95 Å). Moreover, the diazene linker formed one H-bond with *Aspartate1044* (2.47 Å) while NH group of sulfonamide moiety formed a

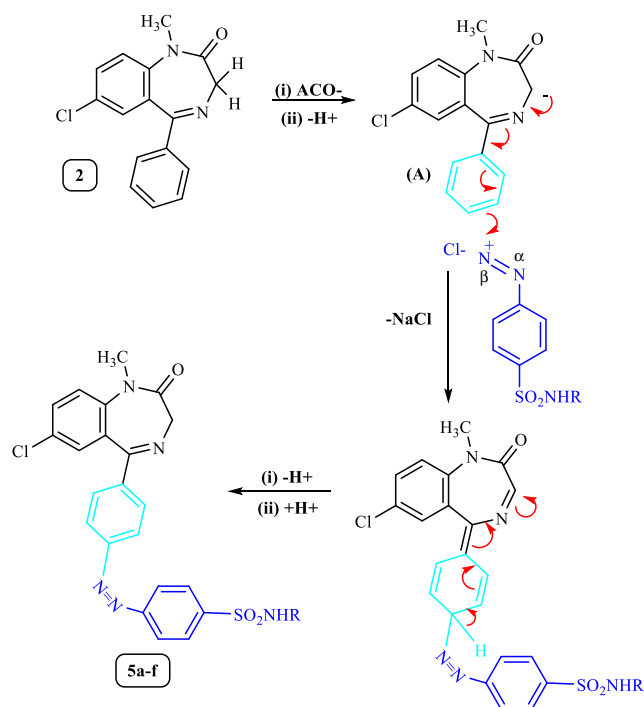


Fig. 6. Proposed mechanism for synthesis of compounds 5a-f.

second H bond with *Aspartate1044* (2.23 Å). Furthermore, the distal quinoxaline moiety was stabilized by formation of two H-bonds with *Arginine1025* (2.17 Å, 2.55 Å). The diazepam scaffold occupied the hydrophobic groove formed by *Leucine1033*, *Glycine920*, *Lysine918*, *Cysteine917*, *Phenylalanine916*, *Glutamate915*, *Alanine864* and *Leucine838*. Moreover, the central phenyldiazene spacer occupied the hydrophobic pocket formed by *Aspartate1044*, *Cysteine1043*, *Leucine1033*, *Glutamate915*, *Valine914*, *Valine897* and *Lysine866*. The hydrophobic phenyl tail occupied the hydrophobic pocket formed by *Aspartate1044*, *Cysteine1043*, *Isoleucine1042*, *Valine897*, *Leucine887*, *Lysine866* and *Glutamate883*. Furthermore, the distal quinoxaline moiety occupied the hydrophobic groove formed by *Arginine1025*, *Histidine1024*, *Isoleucine1023*, *Cysteine1022*, *Lysine1021*, *Arginine1020*, *Leucine1017*, *Isoleucine890*, *Histidine889* and *Isoleucine886* (Fig. 12). These interactions of compound 5f may explain its high anticancer activity.

From the obtained docking results (Table 1), we concluded that, all the synthesized compounds exhibited higher affinities towards VEGFR-2 except compound 5a which showed lower affinity and compounds 7a-c which displayed nearly equipotent affinities in comparing to sorafenib. The diazene linker occupied the same groove occupied by urea linker of **sorafenib** and played the same role which is essential for higher affinity towards VEGFR-2 enzyme. The distal moieties formed Hydrogen and hydrophobic bonding interactions and consequently affinities towards VEGFR-2 enzyme. Elongation of the structure played an important role in their VEGFR-2 inhibitory activities. The diazene and sulfonamide linkers formed hydrogen bonding interactions which increased affinity towards VEGFR-2 enzyme. On the other hand, diazepam scaffold compensated hydrogen bonding and hydrophobic interactions of *N*-methylpicolinamide moiety of sorafenib.

### 2.3. In vitro cytotoxic activity

Anti-proliferative activity of the newly synthesized derivatives 5a-f 7a-c was examined against three human tumor cell lines namely, hepatocellular carcinoma (HepG2), colorectal carcinoma (HCT-116) and breast cancer (MCF-7) using 3-[4,5-dimethylthiazol-2-yl]-2,5-diphenyltetrazolium bromide (MTT) colorimetric assay as described by Mosmann

[49,72–74]. Sorafenib and doxorubicin were included in the experiments as reference cytotoxic drugs. The results were expressed as growth inhibitory concentration (IC<sub>50</sub>) values and summarized in Table 2. From the obtained results, it was explicated that most of the prepared compounds displayed excellent to modest growth inhibitory activity against the tested cancer cell lines. In general, investigations of the cytotoxic activity indicated that MCF-7 was the most sensitive cell line to the influence of the new derivatives respectively. In particular, compound 5d was found to be the most potent derivative overall the tested compounds against the three HepG2, HCT116 and MCF-7 cancer cell lines with IC<sub>50</sub> = 8.98 ± 0.1, 7.77 ± 0.1 and 6.99 ± 0.1 μM respectively. Compound 5d exhibited higher activity than sorafenib, (IC<sub>50</sub> = 9.18 ± 0.6, 5.47 ± 0.3 and 7.26 ± 0.3 μM respectively), against HepG2 and MCF-7 but exhibited lower activity against HCT116 cancer cell lines respectively. Also, this compound displayed lower activity than doxorubicin, (IC<sub>50</sub> = 7.94 ± 0.6, 8.07 ± 0.8 and 6.75 ± 0.4 μM respectively), against HepG2 and MCF-7 but higher activity against HCT116 cell lines respectively.

With respect to the HepG2 hepatocellular carcinoma cell line, compounds 5c, 5f, 5b and 5e displayed very good anticancer activities with (IC<sub>50</sub> = 11.32 ± 0.3, 11.99 ± 0.3, 14.49 ± 0.3 and 16.11 ± 0.3 μM, respectively). Compounds 7c and 7b, with IC<sub>50</sub> = 21.34 ± 1.6 and 23.11 ± 2.2 μM respectively, displayed good cytotoxicity. While compounds 5a and 7a with (IC<sub>50</sub> = 31.76 ± 3.1 and 32.09 ± 2.6 μM) exhibited moderate cytotoxicity.

Cytotoxicity evaluation against colorectal carcinoma (HCT-116) cell line, discovered that compounds 5f and 5c displayed excellent anticancer activities with (IC<sub>50</sub> = 9.33 ± 0.2 and 9.87 ± 0.2 μM, respectively). Compounds 5b, 5e and 7c displayed very good anticancer activities with (IC<sub>50</sub> = 11.39 ± 0.2, 13.23 ± 0.2 and 19.63 ± 1.7 μM, respectively). Compounds 7b and 7a, with IC<sub>50</sub> = 22.21 ± 2.2 and 28.28 ± 2.7 μM respectively, displayed good cytotoxicity. While compound 5a with (IC<sub>50</sub> = 37.34 ± 3.2 μM) exhibited moderate cytotoxicity.

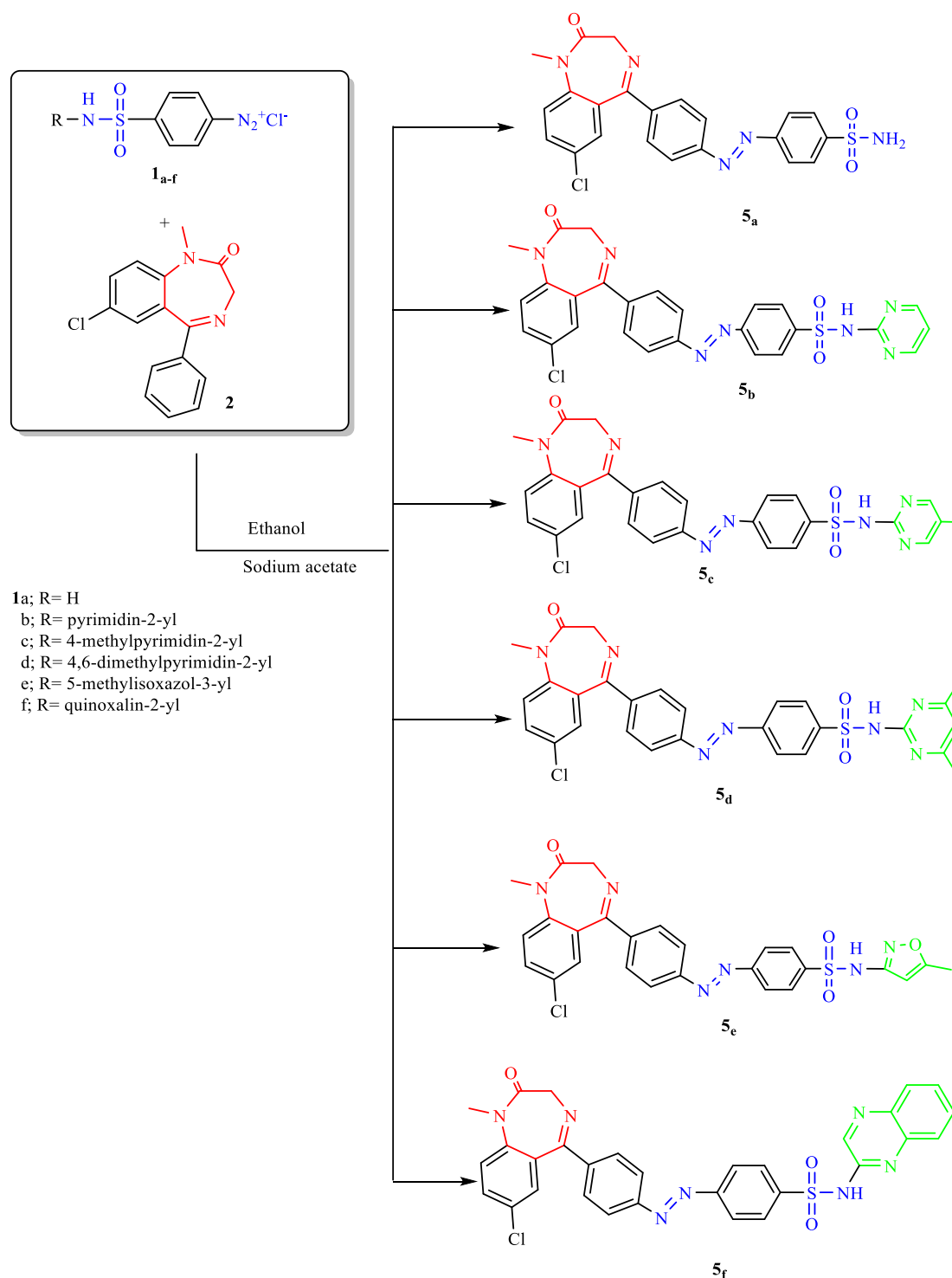
Cytotoxicity evaluation against MCF-7 cell line, revealed that compounds 5c, 5b and 5e displayed excellent anticancer activities with (IC<sub>50</sub> = 7.24 ± 0.2, 8.65 ± 0.2 and 8.87 ± 0.2 μM, respectively). Compounds 5f and 7c displayed very good anticancer activities with (IC<sub>50</sub> = 10.11 ± 0.2 and 17.99 ± 1.6 μM, respectively). Compounds 7b with IC<sub>50</sub> = 20.13 ± 2.2 μM, displayed good cytotoxicity. While compounds 5a and 7a with (IC<sub>50</sub> = 33.10 ± 3.1 and 30.66 ± 2.6 μM) exhibited moderate cytotoxicity.

Finally, the most potent six derivatives 5b, 5c, 5d, 5e, 5f and 7c were tested for their cytotoxicity against normal VERO cell lines. The results revealed that the tested compounds have low toxicity against VERO normal cells with IC<sub>50</sub> values ranging from 41.54 to 66.67 μM. The cytotoxicity of the tested compounds against the cancer cell lines was from 6.99 to 37.34 μM.

Compounds 5b, 5c, 5d, 5e, 5f and 7c are respectively, 5.77, 8.58, 9.54, 5.71, 4.68 and 2.31 fold times more toxic in breast cancer cell lines (MCF-7, the most sensitive cells) than in VERO normal cells.

### 2.4. In vitro VEGFR-2 kinase assay

Furthermore, all the synthesized compounds 5a-f and 7a-c were evaluated for their inhibitory activities against VEGFR-2 by using an anti-phosphotyrosine antibody with the Alpha Screen system (PerkinElmer, USA). The results were reported as a 50% inhibition concentration value (IC<sub>50</sub>) calculated from the concentration-inhibition response curve and summarized in Table 2. Sorafenib was used as positive control in this assay. The tested compounds displayed high to medium inhibitory activity with IC<sub>50</sub> values ranging from 0.10 ± 0.01 to 0.32 ± 0.06 μM. Among them, compound 5d was found to be the most potent derivative that inhibited VEGFR-2 at IC<sub>50</sub> value of 0.10 ± 0.01 μM, which is equipotent to sorafenib IC<sub>50</sub> value (0.10 ± 0.02 μM). Compound 5c exhibited excellent activity with IC<sub>50</sub> value of 0.12 ± 0.01 μM which nearly equipotent to that of sorafenib. Compounds 5b, 5e and 5f exhibited very good activity with the same IC<sub>50</sub> value of 0.14 ± 0.02



**Scheme 1.** Synthetic route for preparation of the target compounds **5a-f**.

$\mu\text{M}$ . Also, compounds **7c** and **7b** possessed good VEGFR-2 inhibition with  $\text{IC}_{50}$  values of  $0.16 \pm 0.06$  and  $0.17 \pm 0.06$   $\mu\text{M}$  respectively which are more than the half activity of that of sorafenib. On the other hand, compounds **7a** and **5a** displayed the moderate VEGFR-2 inhibition with  $\text{IC}_{50}$  values =  $0.29 \pm 0.06$  and  $0.32 \pm 0.06$   $\mu\text{M}$ , respectively.

### 2.5. Structure activity relationship (SAR)

The preliminary SAR study has focused on the effect of replacement of the urea and NH linkers of sorafenib and pazopanib respectively with

diazene linkers which interacting as H-bond acceptors and also sulfonamide linkers which act as H-bond donor through its NH group. These linkers interacting with the side chain NH and carboxylate of the essential amino acid residue *Aspartate1044* respectively. Also hydrophobic interactions through the attached (un)substituted hydrophobic distal moieties. The effect of replacement of pyridine and 2,3-dimethyl-2H-indazole moieties of the reference ligands sorafenib and pazopanib, respectively by the benzodiazepine moiety of diazepam scaffold of the synthesized compounds on the antitumor activities also was noticed. This benzodiazepine moiety occupied the same hydrophobic pocket

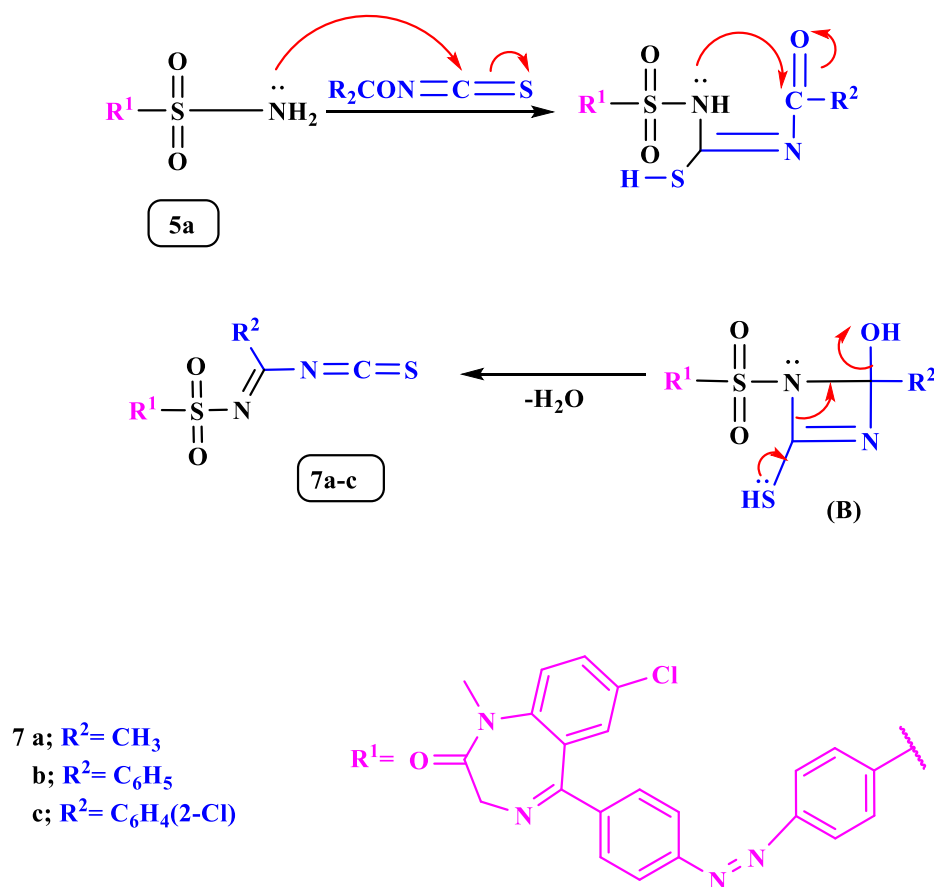
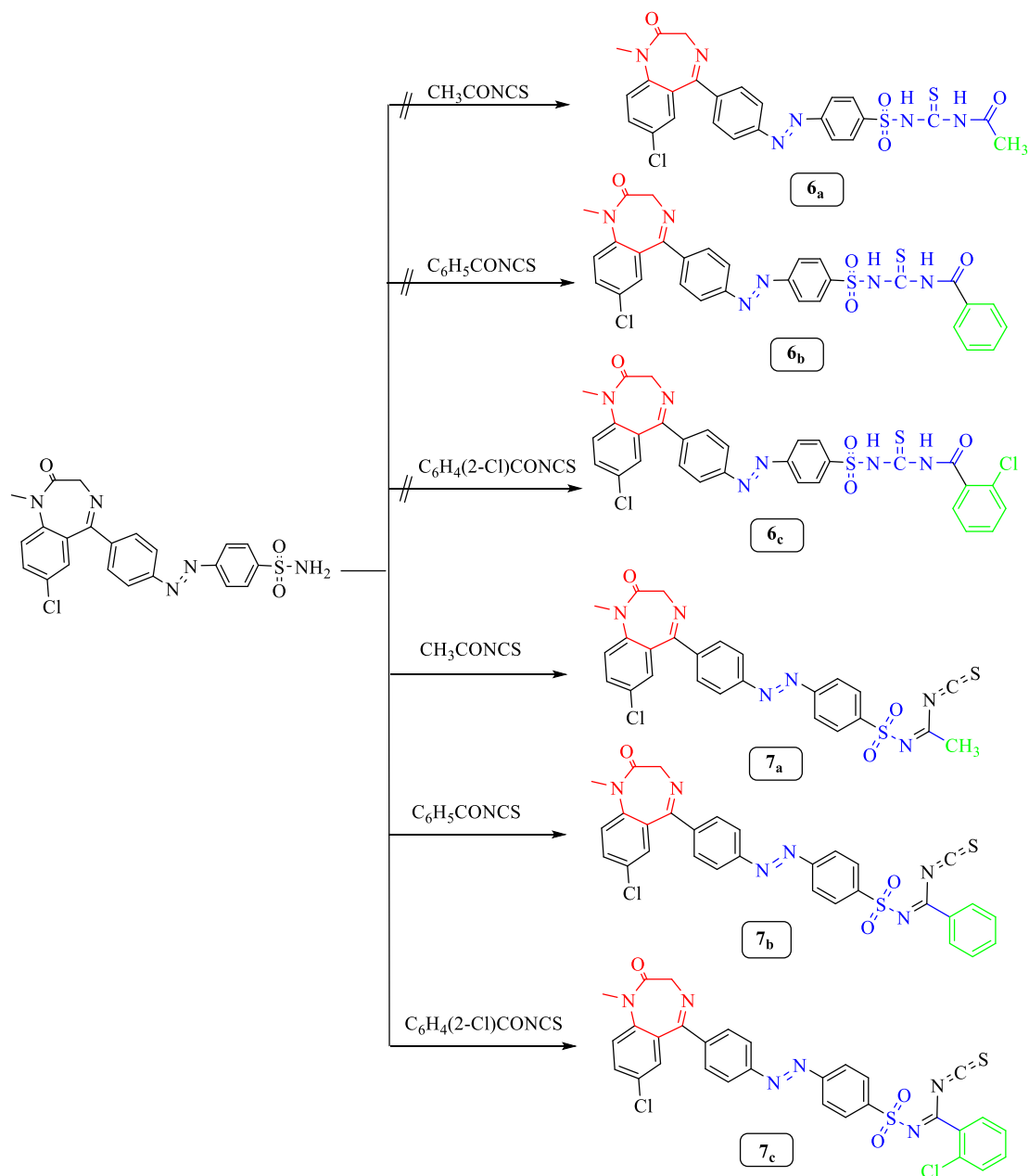


Fig. 7. Proposed mechanism for the formation of compounds 7<sub>a-c</sub>.

which occupied by the pyridine moiety of the standard ligand. Moreover, the phenyldiazeno spacer was designed to replace the central aryl and the methylaminopyrimidine rings of the reference ligands sorafenib and pazopanib, respectively. On the other hand different distal aliphatic, aromatic and heteroaromatic moieties were introduced to the phenyl tail of the reference ligand with different lipophilicity and electronic nature in order to study their effects on the anticancer activity. The presence of lipophilic distal moieties attached to the phenyl ring through sulfonamide linkers in order to increase the length of the structure to enable these distal moieties to form new hydrophobic and H-bonding interactions with the active site. The data obtained revealed that, the tested compounds displayed different levels of anticancer activity and possessed a distinctive pattern of selectivity against the MCF-7 cell lines. Generally, the spacers, linkers (HBA-HBD), lipophilicity and electronic nature exhibited an important role in anticancer activity. The presence of the hydrophobic heteroaromatic distal moieties and the linkers diazene and sulfonamide of compounds 5<sub>a-f</sub> were found to be responsible for their highest anticancer activities than the other compounds 7<sub>a-c</sub> that containing phenyl and/or methyl ones. From the structure of the synthesized derivatives and the data shown in Table 2 we can divide these tested compounds into two groups. The first group is compounds 5<sub>a-f</sub>, the terminal phenyl tail was substituted with different heteroaromatic moieties linked through sulfonamide linkers as in compound 5<sub>b-f</sub>, and the sulfonamide linker was unsubstituted as in compound 5<sub>a</sub>. Generally, the substituted sulfonamide linker as in compounds 5<sub>b-f</sub> displayed higher activities than the unsubstituted one as in compound 5<sub>a</sub> against the three HepG2, HCT116 and MCF-7 cell lines. The presence of distal 4,6-dimethylpyrimidine moiety with two hydrophobic electron donating methyl groups at positions 4 and 6 as in compound 5<sub>d</sub> exhibited higher anticancer activities than the 5-methylpyridine one 5<sub>c</sub> and the unsubstituted pyridine one 5<sub>b</sub> against the three HepG2, HCT116

and MCF-7 cell lines. The distal 4,6-dimethylpyrimidine moiety with two hydrophobic electron donating methyl groups 5<sub>d</sub> exhibited higher anticancer activities than the 5-methylpyridine with hydrophobic electron donating methyl one 5<sub>c</sub> and the pyrazine one fused to the electron deficient benzene ring to form quinoxaline moiety 5<sub>f</sub> against HepG2 and MCF-7 cell lines. While the distal 4,6-dimethylpyrimidine moiety 5<sub>d</sub> exhibited higher anticancer activities than the quinoxaline moiety 5<sub>f</sub> and 5-methylpyridine one 5<sub>c</sub> against HCT116 cell lines respectively. Moreover, the distal six membered heteroaromatic pyrimidine moieties 5<sub>d</sub>, 5<sub>c</sub> and 5<sub>b</sub> exhibited higher anticancer activities than the five heteroaromatic isoxazole one 5<sub>e</sub> against the three HepG2, HCT116 and MCF-7 cell lines. Moreover, the distal six membered heteroaromatic quinoxaline 5<sub>f</sub> exhibited higher anticancer activities than the five heteroaromatic isoxazole one 5<sub>e</sub> against HepG2 and HCT116 cell lines but lower activity against MCF-7 cell lines. In the second group 7<sub>a-c</sub>, the distal electron deficient phenyl ring substituted with hydrophobic electron withdrawing chloro group as in compound 7<sub>c</sub> exhibited higher activities than that unsubstituted phenyl one 7<sub>b</sub> and the aliphatic electron donating methyl one 7<sub>a</sub> against the three HepG2, HCT116 and MCF-7 cell lines.

The data obtained from VEGFR-2 inhibition assay concluded that, generally the distal heteroaromatic 5<sub>b-f</sub> displayed higher activity than the 2-chlorophenyl 7<sub>c</sub>, phenyl 7<sub>b</sub> and/or aliphatic methyl one 7<sub>a</sub> respectively. Also, these distal moieties attached to sulfonamide linkers showed higher activities than the sulfonamide group without any distal moiety 5<sub>a</sub>. The presence of the distal hydrophobic 4,6-dimethylpyrimidine moiety with two hydrophobic electron donating methyl groups at positions 4 and 6 as in compound 5<sub>d</sub> exhibited the highest VEGFR-2 inhibition activity that equipotent to Sorafenib. In addition, 4,6-dimethylpyrimidine moiety exhibited higher activity than that mono substituted with methyl (5-methylpyrimidine) 5<sub>c</sub> and/or the



**Scheme 2.** Synthetic route for preparation of the target compounds **7a-c**.

unsubstituted pyrimidine **5b** respectively. The distal hydrophobic heteroaromatic pyridine **5b**, 5-methylisoxazole **5e** and quinoxaline **5f** exhibited the same VEGFR-2 inhibition activity.

### 3. Conclusion

In summary, nine new diazepam bearing sulfonamide derivatives have been designed, synthesized and evaluated for their anticancer activities against three human tumor cell lines hepatocellular carcinoma (HepG2), colorectal carcinoma (HCT-116) and breast cancer (MCF-7) targeting VEGFR-2 enzyme. All the tested compounds showed variable anticancer activities. The molecular design was performed to investigate the binding mode of the proposed compounds with VEGFR-2 receptor. The diazene and/or sulfonamide linkers played the same role of urea linker of **sorafenib** which is essential for higher affinity towards VEGFR-2 enzyme. The diazepam scaffold increased hydrophobic interactions and form H-bond through its carbonyl group at position-2 with the

amino acid *Cysteine917*. The distal moieties formed new hydrogen and hydrophobic bonding interactions and consequently affinities towards VEGFR-2 enzyme. Elongation of the structure played an important role in their VEGFR-2 inhibitory activities. The data obtained from the docking studies were highly correlated with that obtained from the biological screening. All the tested compounds showed variable anticancer activities. MCF-7 was the most sensitive cell line to the influence of the new derivatives. In particular, compound **5d** was found to be the most potent derivative overall the tested compounds against the three HepG2, HCT116 and MCF-7 cancer cell lines with  $\text{IC}_{50} = 8.98 \pm 0.1$ ,  $7.77 \pm 0.1$  and  $6.99 \pm 0.1 \mu\text{M}$  respectively. Compound **5d** exhibited higher activity than sorafenib, ( $\text{IC}_{50} = 9.18 \pm 0.6$ ,  $5.47 \pm 0.3$  and  $7.26 \pm 0.3 \mu\text{M}$  respectively), against HepG2 and MCF-7 but exhibited lower activity against HCT116 cancer cell lines respectively. Also, this compound displayed lower activity than doxorubicin, ( $\text{IC}_{50} = 7.94 \pm 0.6$ ,  $8.07 \pm 0.8$  and  $6.75 \pm 0.4 \mu\text{M}$  respectively), against HepG2 and MCF-7 but higher activity against HCT116 cell lines respectively. Compounds

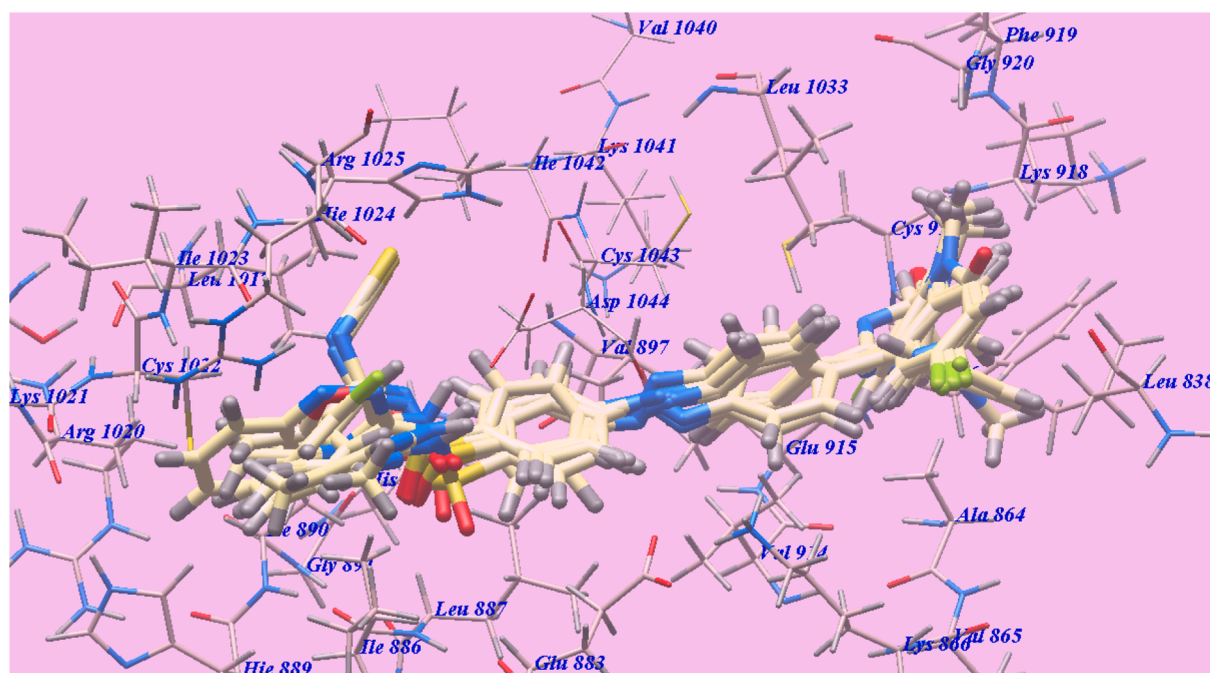


Fig. 8. Superimposition of some docked compounds inside the binding pocket of 1YWN.

Table 1

The calculated free energy of binding ( $\Delta G$  in Kcal/mole) for the ligands.

Compound	$\Delta G$ [kcal mol <sup>-1</sup> ]	Compound	$\Delta G$ [kcal mol <sup>-1</sup> ]
5 <sub>a</sub>	-84.43	5 <sub>f</sub>	-101.97
5 <sub>b</sub>	-101.84	7 <sub>a</sub>	-90.48
5 <sub>c</sub>	-107.58	7 <sub>b</sub>	-92.86
5 <sub>d</sub>	-116.78	7 <sub>c</sub>	-95.46
5 <sub>e</sub>	-100.75	Sorafenib	-95.66

5<sub>b</sub>, 5<sub>c</sub>, 5<sub>d</sub>, 5<sub>e</sub>, 5<sub>f</sub> and 7<sub>c</sub> are respectively, 5.77, 8.58, 9.54, 5.71, 4.68 and 2.31 fold times more toxic in breast cancer cell lines (MCF-7, the most sensitive cells) than in VERO normal cells. All the synthesized compounds 5<sub>a-f</sub> and 7<sub>a-c</sub> were evaluated for their inhibitory activities against VEGFR-2. Among them, compound 5<sub>d</sub> was found to be the most potent derivative that inhibited VEGFR-2 at IC<sub>50</sub> value of 0.10 ± 0.01 μM, which is equipotent to sorafenib IC<sub>50</sub> value (0.10 ± 0.02 μM). Compound 5<sub>c</sub> exhibited excellent activity with IC<sub>50</sub> value of 0.12 ± 0.01 μM which nearly equipotent to that of sorafenib. Compounds 5<sub>b</sub>, 5<sub>e</sub> and 5<sub>f</sub> exhibited very good activity with the same IC<sub>50</sub> value of 0.14 ± 0.02 μM. Also, compounds 7<sub>c</sub> and 7<sub>b</sub> possessed good VEGFR-2 inhibition with IC<sub>50</sub> values of 0.16 ± 0.06 and 0.17 ± 0.06 μM respectively which are more than the half activity of that of sorafenib. On the other hand, compounds 7<sub>a</sub> and 5<sub>a</sub> displayed the moderate VEGFR-2 inhibition with IC<sub>50</sub> values = 0.29 ± 0.06 and 0.32 ± 0.06 μM, respectively. The obtained results showed that, our compounds could be useful as a template for future design, optimization and investigation to produce more potent and selective VEGFR-2 inhibitors with higher anticancer analogs with lower side effects.

## 4. Experimental

### 4.1. Chemistry

#### 4.1.1. General

All melting points of the synthesized compounds were recorded on Büchi melting point apparatus D-545. IR spectra (KBr disks) were measured on an FTIR plus 460 or Pye Unicam SP-1000 spectrophotometer (Pye Unicam, Cambridge, UK). <sup>1</sup>H NMR spectra were obtained

using BRUKER (400 MHz, Varian, UK) using DMSO-*d*<sub>6</sub> as a solvent and tetraethylsilane (TMS) as internal standard chemical shifts are expressed as δ ppm. <sup>13</sup>C NMR (100 MHz) spectra, using DMSO-*d*<sub>6</sub> as a solvent and TMS (δ) as the internal standard. Analytical data were obtained from Vario EL III Elemental CHNS analyzer.

#### 4.1.2. General procedure for synthesis of target compounds (5<sub>a-f</sub>)

The appropriate 4-Aminobenzenesulfonamide derivative (0.01 mol) was suspended in water (50 mL). HCl (10 mL, 36.5%) was added drop wise to this solution with stirring. The mixture was gradually heated up to 30 °C till a clear solution was obtained. The solution was cooled to 0–5 °C in an ice bath. A sodium nitrite solution (0.5 g in 5 mL H<sub>2</sub>O) was then added over a period of 5 min while stirring to obtain diazonium salt solution. Diazepam (2.85 gm, 0.01 mol) was dissolved in ethanol in the presence of sodium acetate and kept at 0–5 °C. Subsequently, the diazonium salt solution was added with the occasional slow stirring to the diazepam solution for 10–15 min. The formed precipitate was filtered, dried, and washed with ethanol to give the corresponding derivatives 5<sub>a-f</sub> respectively.

4.1.2.1. 4-([4-{7-Chloro-1-methyl-2-oxo-2,3-dihydro-1H-benzof[e][1,4]diazepin-5-yl}phenyl]diazanyl)benzene-5<sub>a</sub>). Red crystals; m.p. 110–112 °C; yield 93%; IR (KBr, cm<sup>-1</sup>): 3468, 3396 (NH<sub>2</sub>), 1685 (C=O), 1597 (N=N), 1315, 1156 (SO<sub>2</sub>); <sup>1</sup>H NMR (DMSO-*d*<sub>6</sub>) δ: 3.30 (s, 3H, N-CH<sub>3</sub>), 3.92 (d, 1H, J = 10.8, CH methylene), 4.59 (d, 1H, J = 10.8, CH methylene), 4.88 (s br, 2H, NH<sub>2</sub>, D<sub>2</sub>O exchangeable), 7.25 (d, 1H, J = 2.4, C<sub>6</sub>H<sub>3</sub>), 7.49 (d, 2H, J = 7.6, C<sub>6</sub>H<sub>4</sub>-SO<sub>2</sub>), 7.53 (d, 2H, J = 7.6, C<sub>6</sub>H<sub>4</sub>-SO<sub>2</sub>), 7.58 (s, 2H, NH<sub>2</sub>, D<sub>2</sub>O exchangeable), 7.61 (d, 2H, J = 8.3, C<sub>6</sub>H<sub>4</sub>-N<sub>2</sub>), 7.67 (d, 2H, J = 8.3, C<sub>6</sub>H<sub>4</sub>-N<sub>2</sub>), 7.78 (d, 1H, J = 2.4, C<sub>6</sub>H<sub>3</sub>), 7.80 (d, 1H, J = 2.4, C<sub>6</sub>H<sub>3</sub>). <sup>13</sup>C NMR (DMSO-*d*<sub>6</sub>) δ (ppm): 34.15 (CH<sub>3</sub>-N), 55.91 (CH<sub>2</sub>), 119.44 (2), 122.48, 122.83 (2), 128.58 (2), 129.84 (2), 130.52, 130.99, 131.18, 131.38, 139.62, 141.16, 141.40, 151.19, 152.70, 168.38 (C=N), 168.69 (C=O); MS (*m/z*): 467.33 (M<sup>+</sup>, 14.11%), 284.09 (66.74%), 218.44 (60.85%), 216.33 (70.17%), 153.56 (100%, base peak), 133.32 (66.98%); Anal. Calcd for C<sub>22</sub>H<sub>18</sub>ClN<sub>5</sub>O<sub>3</sub>S (467.93): C, 56.47; H, 3.88; N, 14.97; S, 6.85. Found: C, 56.40; H, 3.70; N, 14.80; S, 6.70.

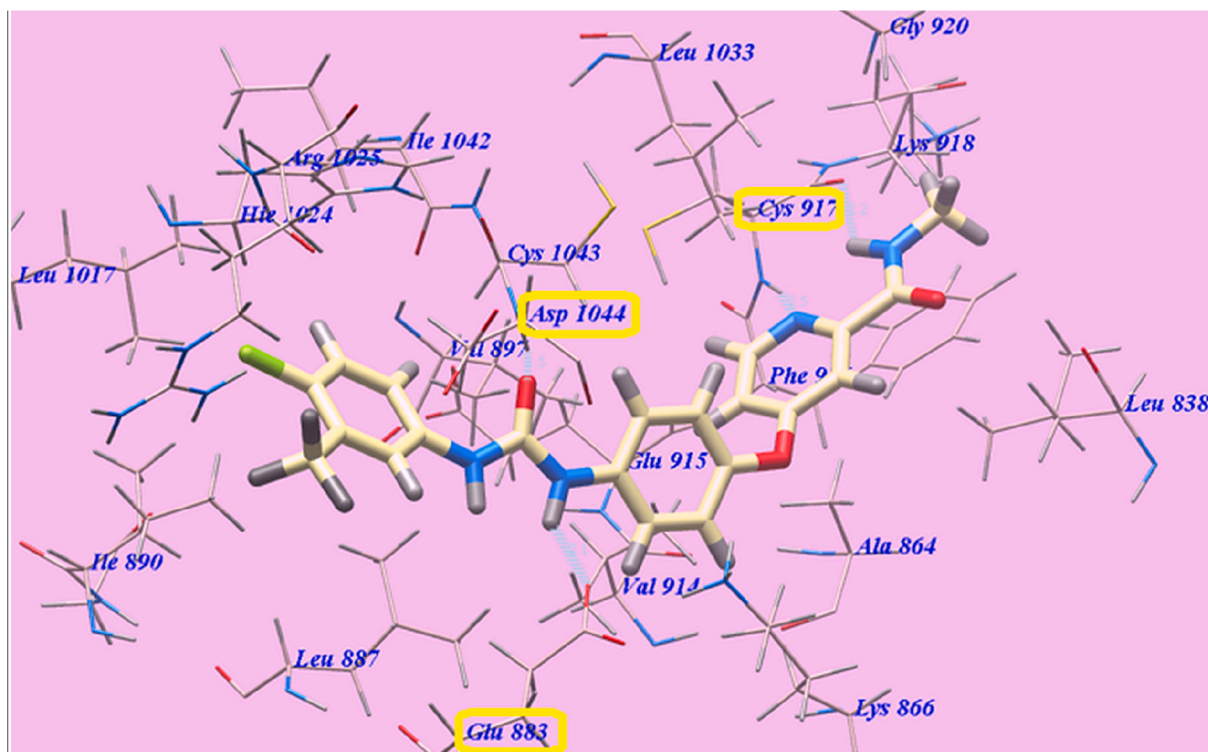


Fig. 9. Predicted binding mode for sorafenib with 1WYN. H-bonded atoms are indicated by dotted lines.

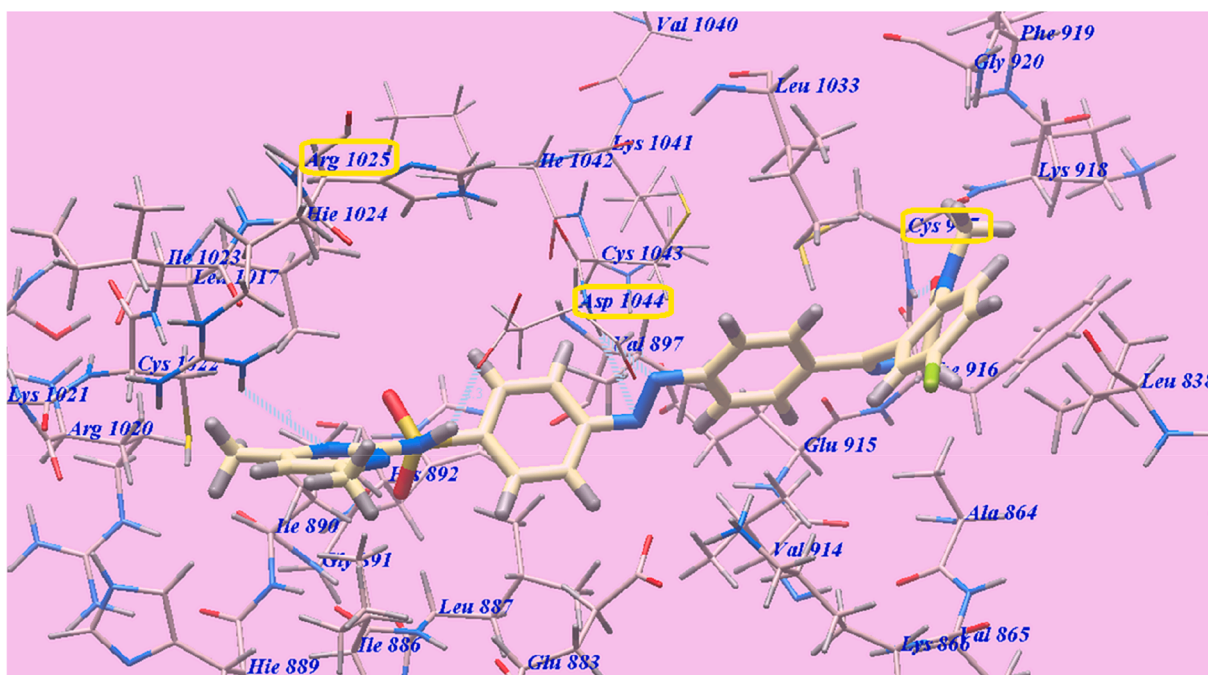


Fig. 10. Predicted binding mode for 5<sub>a</sub> with 1WYN.

4.1.2.2. 4-([4-{7-Chloro-1-methyl-2-oxo-2,3-dihydro-1H-benzo[e][1,4] diazepin-5-yl}phenyl]-diazenyl)-N-(pyrimidin-2-yl)benzenesulfonamide (5<sub>b</sub>). Yellow crystals; m.p. 140–142 °C; yield 85%; IR (KBr, cm<sup>-1</sup>): 3422 (NH), 1685 (C=O), 1603 (N=N), 1314, 1127 (SO<sub>2</sub>); <sup>1</sup>H NMR (DMSO-*d*<sub>6</sub>) δ: 3.27 (s, 3H, N-CH<sub>3</sub>), 3.80 (d, 1H, J = 10.8, CH methylene), 4.60 (d, 1H, J = 10.8, CH methylene), 7.22–7.44 (dd, 3H, J = 7.4, 2.4, CH pyrimidine), 7.46 (d, 1H, J = 7.4, C<sub>6</sub>H<sub>3</sub>), 7.48 (d, 2H, J = 7.4, C<sub>6</sub>H<sub>4</sub>-SO<sub>2</sub>), 7.5 (d, 2H, J = 7.4, C<sub>6</sub>H<sub>4</sub>-SO<sub>2</sub>), 7.54 (d, 2H, J = 8.3, C<sub>6</sub>H<sub>4</sub>-N<sub>2</sub>), 7.60

(d, 2H, J = 8.3, C<sub>6</sub>H<sub>4</sub>-N<sub>2</sub>), 7.7 (d, 1H, J = 2.4, C<sub>6</sub>H<sub>3</sub>), 7.72 (d, 1H, J = 2.4, C<sub>6</sub>H<sub>3</sub>), 8.53 (s, 1H, NH, D<sub>2</sub>O exchangeable). <sup>13</sup>C NMR (DMSO-*d*<sub>6</sub>) δ (ppm): 34.15 (CH<sub>3</sub>-N), 55.91 (CH<sub>2</sub>), 119.98 (2), 121.51 (2), 122.48, 122.83 (2), 129.52 (2), 129.84 (2), 130.52 (2), 130.99 (2), 131.18 (2), 152.70, 154.34 (2), 155.60 (C=N diazepine), 155.73 (C=N pyrimidine), 168.38 (C=N pyrimidine), 168.69 (C=O); MS (*m/z*): 546.03 (M<sup>+</sup>, 12.48%), 509.06 (59.50%), 310.36 (76.40%), 144.12 (78.00%), 119.93 (100%, base peak), 117.33 (81.11%); Anal. Calcd for C<sub>26</sub>H<sub>20</sub>ClN<sub>7</sub>O<sub>3</sub>S

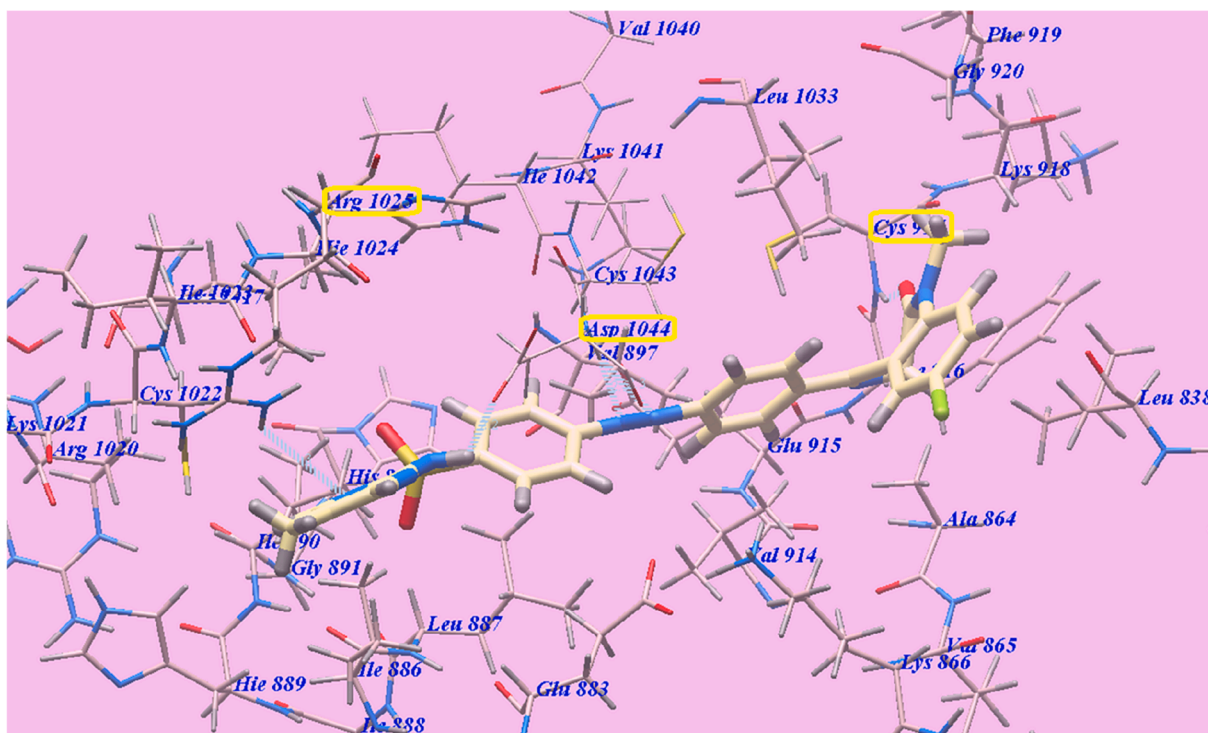


Fig. 11. Predicted binding mode for  $5_c$  with 1WYN.

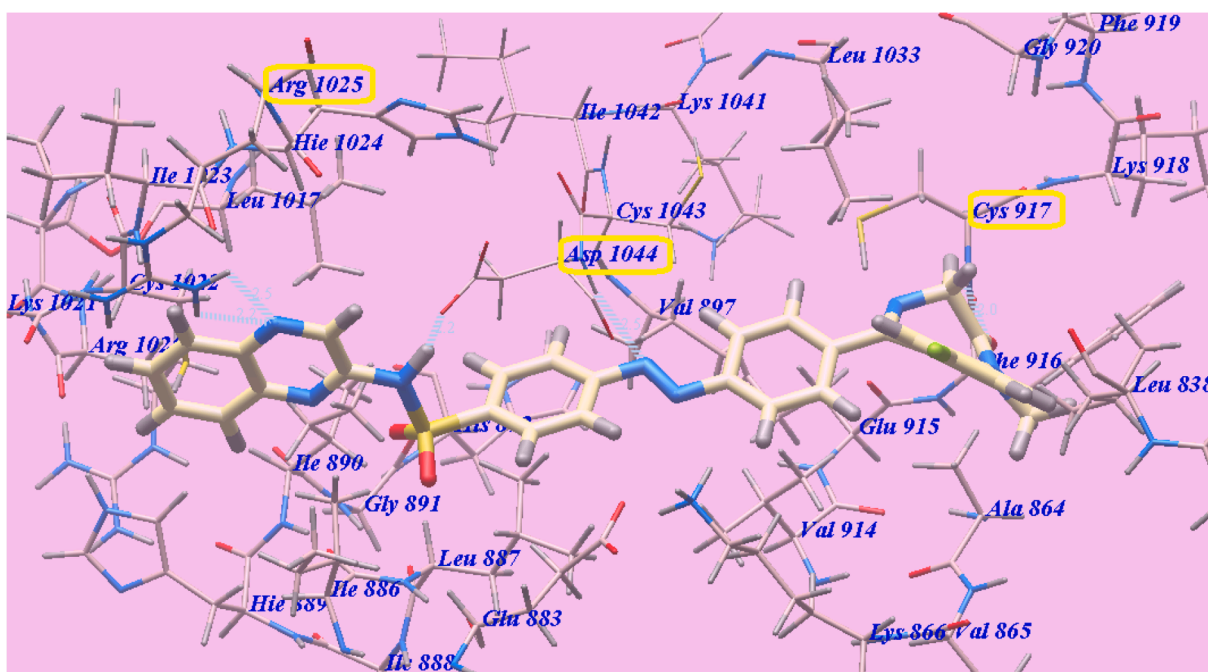


Fig. 12. Predicted binding mode for  $5_f$  with 1WYN.

(546.0): C, 57.20; H, 3.69; N, 17.96; S, 5.87. Found: C, 57.30; H, 3.50; N, 17.90; S, 5.75.

4.1.2.3. 4-([4-{7-Chloro-1-methyl-2-oxo-2,3-dihydro-1H-benzo[e][1,4]diazepin-5-yl}phenyl]diazanyl)-N-(5-methylpyrimidin-2-yl)benzenesulfonamide ( $5_c$ ). Orange crystals; m.p. 135–137 °C; yield 93%; IR (KBr,  $\text{cm}^{-1}$ ): 3441 (NH), 1685 (C=O), 1603 (N=N), 1315, 1166 ( $\text{SO}_2$ );  $^1\text{H}$  NMR (DMSO- $d_6$ )  $\delta$ : 2.51 (s, 3H,  $\text{CH}_3$ ), 3.28 (s, 3H, N- $\text{CH}_3$ ), 3.81 (d, 1H, J = 10.6, CH methylene), 4.60 (d, 1H, J = 10.6, CH methylene), 7.22–7.44

(dd, J = 7.6, 2H, CH pyrimidine), 7.44 (s, 1H,  $\text{C}_6\text{H}_3$ ), 7.46 (d, 2H, J = 7.8,  $\text{C}_6\text{H}_4\text{-SO}_2$ ), 7.51 (d, 2H, J = 7.7,  $\text{C}_6\text{H}_4\text{-SO}_2$ ), 7.56 (d, 2H, J = 8.3,  $\text{C}_6\text{H}_4\text{-N}_2$ ), 7.62 (d, 2H, J = 8.3,  $\text{C}_6\text{H}_4\text{-SO}_2$ ), 7.70 (d, 1H,  $\text{C}_6\text{H}_3$ ), 7.73 (d, 1H,  $\text{C}_6\text{H}_3$ ), 8.5 (s, 1H, NH,  $\text{D}_2\text{O}$  exchangeable);  $^{13}\text{C}$  NMR (DMSO- $d_6$ )  $\delta$  (ppm): 16.14 ( $\text{CH}_3$ ), 34.76 ( $\text{CH}_3\text{-N}$ ), 55.91 ( $\text{CH}_2$ ), 119.98 (2), 122.48 (2), 122.65 (2), 122.83 (2), 129.52 (2), 129.84 (2), 130.52, 130.99 (2), 131.18 (2), 153.34 (2), 155.58, 156.48 (C=N diazepine), 159.79 (C=N pyrimidine), 168.38 (C=N pyrimidine), 168.69 (C=O); MS ( $m/z$ ): 560.52 ( $\text{M}^+$ , 18.89%), 506.74 (51.07%), 487.13 (100%, base peak),

Table 2

*In vitro* cytotoxic activities of the newly synthesized compounds against HepG2, HCT-116, MCF-7 and VERO cell lines and VEGFR-2 kinase assay.

Compound	IC <sub>50</sub> (μM) <sup>a</sup>				
	HepG2	HCT116	MCF-7	VERO	VEGFR-2
5 <sub>a</sub>	31.76 ± 3.1	37.34 ± 3.2	33.10 ± 3.1	<sup>b</sup> NT	0.32 ± 0.06
5 <sub>b</sub>	14.49 ± 0.3	11.39 ± 0.2	8.65 ± 0.2	49.88 ± 0.22	0.14 ± 0.02
5 <sub>c</sub>	11.32 ± 0.3	9.87 ± 0.2	7.24 ± 0.2	62.12 ± 0.18	0.12 ± 0.01
5 <sub>d</sub>	8.98 ± 0.1	7.77 ± 0.1	6.99 ± 0.1	66.67 ± 0.21	0.10 ± 0.01
5 <sub>e</sub>	16.11 ± 0.3	13.23 ± 0.2	8.87 ± 0.2	50.61 ± 0.22	0.14 ± 0.02
5 <sub>f</sub>	11.99 ± 0.3	9.33 ± 0.2	10.11 ± 0.2	47.31 ± 0.22	0.14 ± 0.02
7 <sub>a</sub>	32.09 ± 2.6	28.28 ± 2.7	30.66 ± 2.6	<sup>b</sup> NT	0.29 ± 0.06
7 <sub>b</sub>	23.11 ± 2.2	22.21 ± 2.2	20.13 ± 2.2	<sup>b</sup> NT	0.17 ± 0.06
7 <sub>c</sub>	21.34 ± 1.6	19.63 ± 1.7	17.99 ± 1.6	41.54 ± 0.22	0.16 ± 0.06
Sorafenib	9.18 ± 0.6	5.47 ± 0.3	7.26 ± 0.3	<sup>b</sup> NT	0.10 ± 0.02
Doxorubicin	7.94 ± 0.6	8.07 ± 0.8	6.75 ± 0.4	<sup>b</sup> NT	<sup>b</sup> NT

<sup>a</sup> IC<sub>50</sub> values are the mean ± S.D. of three separate experiments.

<sup>b</sup> NT: Compounds not tested.

477.16 (43.72%), 439.40 (94.81%), 129.68 (83.22%); Anal. Calcd for: C<sub>27</sub>H<sub>22</sub>ClN<sub>7</sub>O<sub>3</sub>S (560.03): C, 57.91; H, 3.96; N, 17.51; S, 5.72. Found: C, 57.90; H, 3.80; N, 17.50; S, 5.40.

4.1.2.4. 4-([4-{7-Chloro-1-methyl-2-oxo-2,3-dihydro-1H-benzo[e][1,4] diazepin-5-yl}phenyl]diazanyl)-N-(4,6-dimethylpyrimidin-2-yl)benzenesulfonamide (5<sub>d</sub>). Red crystals; m.p. 115–117 °C; yield 94%; IR (KBr, cm<sup>-1</sup>): 3419 (NH), 1685 (C=O), 1596 (N=N), 1314, 1143 (SO<sub>2</sub>); <sup>1</sup>H NMR (DMSO-*d*<sub>6</sub>) δ: 2.24 (s, 6H, 2CH<sub>3</sub> pyrimidine), 3.34 (s, 3H, N-CH<sub>3</sub> diazepine), 3.81 (d, 1H J = 10.6, CH methylene), 4.60 (d, 1H J = 10.6, CH methylene), 6.75 (s, 1H, CH pyrimidine), 7.22 (s, 1H, C<sub>6</sub>H<sub>3</sub>), 7.45 (d, 2H, J = 7.62, C<sub>6</sub>H<sub>4</sub>-SO<sub>2</sub>), 7.53 (d, 2H, J = 7.0, C<sub>6</sub>H<sub>4</sub>-N<sub>2</sub>), 7.57 (d, 2H, J = 7.0, C<sub>6</sub>H<sub>4</sub>-N<sub>2</sub>), 7.63 (d, 3H, J = 7.7, C<sub>6</sub>H<sub>4</sub>-SO<sub>2</sub>), 7.71 (d, 1H, C<sub>6</sub>H<sub>3</sub>), 7.73 (d, 1H, J = 2.2, C<sub>6</sub>H<sub>3</sub>), 11.97 (s, 1H, NH, D<sub>2</sub>O exchangeable); <sup>13</sup>C NMR (DMSO-*d*<sub>6</sub>) δ (ppm): 19.40 (2CH<sub>3</sub>), 34.76 (CH<sub>3</sub>-N), 57.15 (CH<sub>2</sub>), 124.31 (2), 128.22 (2), 128.87 (2), 129.32, 129.61 (2), 129.93 (2), 131.07 (2), 131.89, 138.41, 143.04, 143.76, 144.25, 146.75, 153.86, 154.25 (CN diazepine), 168.53 (2C = N pyrimidine), 169.65 (C=O); Anal. Calcd for: C<sub>28</sub>H<sub>24</sub>ClN<sub>7</sub>O<sub>3</sub>S (574.06): C, 58.58; H, 4.21; N, 17.08; S, 5.58 Found: C, 58.50; H, 4.20; N, 17.00; S, 5.60.

4.1.2.5. 4-([4-{7-Chloro-1-methyl-2-oxo-2,3-dihydro-1H-benzo[e][1,4] diazepin-5-yl}phenyl]diazanyl)-N-(5-methylisoxazol-3-yl)benzenesulfonamide (5<sub>e</sub>). Red crystals; m.p. 130–132 °C; yield 92%; IR (KBr, cm<sup>-1</sup>): 3419 (NH), 1685 (C=O), 1596 (N=N), 1341, 1128 (SO<sub>2</sub>); <sup>1</sup>H NMR (DMSO-*d*<sub>6</sub>) δ: 2.30 (s, 3H, CH<sub>3</sub>), 3.39 (s, 3H, N-CH<sub>3</sub>), 3.82 (d, 1H, J = 10.8, CH methylene), 4.60 (d, 1H, J = 10.8, CH methylene), 6.16 (d, 2H, J = 7.6, C<sub>6</sub>H<sub>4</sub>-SO<sub>2</sub>), 6.60 (s, 1H, CH isoxazole), 7.46 (d, 2H, J = 7.6, C<sub>6</sub>H<sub>4</sub>-SO<sub>2</sub>), 7.51 (s, 1H, C<sub>6</sub>H<sub>3</sub>), 7.55 (d, 2H, J = 8.2, C<sub>6</sub>H<sub>4</sub>-N<sub>2</sub>), 7.63 (d, 2H, J = 8.3, C<sub>6</sub>H<sub>4</sub>-N<sub>2</sub>), 7.71 (d, 1H, C<sub>6</sub>H<sub>3</sub>), 7.74 (d, 1H, J = 2.4, C<sub>6</sub>H<sub>3</sub>), 10.9 (s, 1H, NH, D<sub>2</sub>O exchangeable); <sup>13</sup>C NMR (DMSO-*d*<sub>6</sub>) δ (ppm): 15.60 (CH<sub>3</sub>), 34.78 (CH<sub>3</sub>-N), 57.04 (CH<sub>2</sub>), 65.38, 95.75, 95.88, 113.09, 124.31, 124.64, 128.26, 128.89, 129.29, 129.37, 129.66, 129.86, 131.15, 131.96, 138.30, 143.04, 153.72, 157.98, 158.40, 168.68, 169.63, 170.35, 170.83 (C=O); MS (*m/z*): 549.40 (M<sup>+</sup>, 37.55%), 524.77 (70.18%), 465.58 (100%, base peak), 322.20 (48.68%), 272.14 (50.19%); Anal. Calcd for: C<sub>26</sub>H<sub>21</sub>ClN<sub>6</sub>O<sub>4</sub>S (549.00): C, 56.88; H, 3.86; N, 15.31; S, 5.84. Found: C, 56.80; H, 3.70; N, 15.30; S, 5.80.

4.1.2.6. 4-([4-{7-Chloro-1-methyl-2-oxo-2,3-dihydro-1H-benzo[e][1,4] diazepin-5-yl}phenyl]diazanyl)-N-(quinoxalin-2-yl)benzenesulfonamide (5<sub>f</sub>). Orange crystals; m.p. 160–162 °C; yield 90%; IR (KBr, cm<sup>-1</sup>): 3419 (NH), 1685 (C=O), 1596 (N=N), 1314, 1130 (SO<sub>2</sub>); <sup>1</sup>H NMR (DMSO-*d*<sub>6</sub>) δ: 3.35 (s, 3H, N-CH<sub>3</sub>), 3.80 (d, 1H, J = 10.8 Hz, CH methylene), 4.60 (d, 1H, J = 10.8 Hz, CH methylene), 6.07 (s, 1H, J = 8.4 Hz, C<sub>6</sub>H<sub>3</sub>), 6.61 (d, 2H, quinoxaline), 7.22 (s, 1H, C<sub>6</sub>H<sub>3</sub>), 7.50 (d, 2H, J = 7.4, C<sub>6</sub>H<sub>4</sub>-SO<sub>2</sub>), 7.56 (d, 2H, J = 7.2, C<sub>6</sub>H<sub>4</sub>-SO<sub>2</sub>), 7.62 (d, 2H, J = 8.3, C<sub>6</sub>H<sub>4</sub>-N<sub>2</sub>), 7.73 (d, 2H, J = 8.3, C<sub>6</sub>H<sub>4</sub>-N<sub>2</sub>), 7.76–7.93 (m, 2H, quinoxaline), 8.13 (d, 1H, J = 8.4, C<sub>6</sub>H<sub>3</sub>), 8.58 (s, 1H, quinoxaline), 11.3 (s, 1H, NH, D<sub>2</sub>O exchangeable); <sup>13</sup>C NMR (DMSO-*d*<sub>6</sub>) δ (ppm): 34.76 (CH<sub>3</sub>-N), 57.14 (CH<sub>2</sub>), 112.75, 124.25 (2), 124.54, 127.06, 127.57 (2), 128.23, 128.85, 129.14, 129.32 (2), 129.61, 129.90, 130.54, 131.06, 131.14, 131.88 (2), 138.40, 139.09 (2), 139.76, 143.00, 146.75, 153.86, 168.54 (CN), 169.65 (C=O); MS (*m/z*): 596.80 (M<sup>+</sup>, 23.95%), 579.90 (92.63%), 392.23 (100%, base peak), 310.68 (68.16%), 207.49 (82.58%), 200.58 (87.11%); Anal. Calcd for: C<sub>30</sub>H<sub>22</sub>ClN<sub>7</sub>O<sub>3</sub>S (596.06): C, 60.45; H, 3.72; N, 16.45; S, 5.38. Found: C, 60.40; H, 3.70; N, 16.34; S, 5.31.

#### 4.1.3. General procedure for synthesis of target compounds (7<sub>a-c</sub>)

A solution of acid chloride (0.005 mol) and ammonium thiocyanate (0.01 mol) in acetone (15 mL) was heated under reflux for 10 min to obtain acyl isothiocyanate solution. After the reaction mixture was cooled to room temperature and the formed precipitate (NH<sub>4</sub>Cl) was filtered off. To the filtrate of the freshly prepared solution of acylisothiocyanate, sulfanilamide 5<sub>a</sub> (0.86 gm, 0.005 mol) was added, and the mixture was stirred at room temperature for 10 min, the formed precipitate was filtered and washed with acetone to yield the corresponding target compounds, 7<sub>a-c</sub> respectively.

4.1.3.1. N-([4-{ (4-[7-Chloro-1-methyl-2-oxo-2,3-dihydro-1H-benzo[e][1,4] diazepin-5-yl}phenyl]diazanyl)-phenyl]sulfonyl)acetimidoyl isothiocyanate (7<sub>a</sub>). Yellow crystals; m.p. 140–142 °C; yield 82%; IR (KBr, cm<sup>-1</sup>): 2059 (N=C=S), 1693 (C=O), 1597 (N=N), 1343, 1134 (SO<sub>2</sub>); <sup>1</sup>H NMR (DMSO-*d*<sub>6</sub>) δ: 2.09 (CH<sub>3</sub>), 3.35 (s, 3H, N-CH<sub>3</sub>), 3.92 (d, 1H, J = 10.8, CH methylene), 4.59 (d, 1H, J = 10.8, CH methylene), 7.26 (s, 1H, C<sub>6</sub>H<sub>3</sub>), 7.55 (d, 2H, J = 7.6, C<sub>6</sub>H<sub>4</sub>-SO<sub>2</sub>), 7.63 (d, 2H, J = 7.6, C<sub>6</sub>H<sub>4</sub>-SO<sub>2</sub>), 7.66 (d, 2H, J = 8.3, C<sub>6</sub>H<sub>4</sub>-N<sub>2</sub>), 7.77 (d, 2H, J = 8.3, C<sub>6</sub>H<sub>4</sub>-N<sub>2</sub>), 7.85 (d, 2H, C<sub>6</sub>H<sub>3</sub>). <sup>13</sup>C NMR (DMSO-*d*<sub>6</sub>) (ppm) δ: 25.60 (CH<sub>3</sub>), 34.78 (CH<sub>3</sub>-N), 57.04 (CH<sub>2</sub>), 95.75, 95.88, 113.29, 124.37, 124.66, 128.86, 128.89, 129.29, 129.37, 129.66, 129.86, 131.15, 131.96, 138.30, 143.31, 153.64, 157.26 (NCS), 158.89, 168.68, 169.63, 170.35, 170.83 (C=O); MS (*m/z*): 552.58 (M<sup>+</sup>, 68.96%), 438.49 (33.35%), 437.68 (58.38%), 73.47 (55.84%), 71.90 (100%, base peak); Anal. Calcd for: C<sub>25</sub>H<sub>19</sub>ClN<sub>6</sub>O<sub>3</sub>S (551.06): C, 54.49; H, 3.48; N, 15.25; S, 11.64. Found: C, 54.40; H, 3.40; N, 15.20; S, 11.60.

4.1.3.2. N-([4-{ (4-[7-Chloro-1-methyl-2-oxo-2,3-dihydro-1H-benzo[e][1,4] diazepin-5-yl}phenyl]diazanyl) phenyl]sulfonyl)benzimidoyl isothiocyanate (7<sub>b</sub>). Brown crystals; m.p. 215–217 °C; yield 83%; IR (KBr, cm<sup>-1</sup>): 2129 (N=C=S), 1665 (C=O), 1593 (N=N), 1311, 1138 (SO<sub>2</sub>); <sup>1</sup>H NMR (DMSO-*d*<sub>6</sub>) δ: 3.26 (s, 3H, N-CH<sub>3</sub>), 3.73 (d, 1H, J = 10.8, CH methylene), 4.55 (d, 1H, J = 10.8, CH methylene), 7.11 (s, 1H, C<sub>6</sub>H<sub>3</sub>), 7.43 (d, 2H, J = 7.6, C<sub>6</sub>H<sub>4</sub>-SO<sub>2</sub>), 7.48 (d, 2H, J = 7.6, C<sub>6</sub>H<sub>4</sub>-SO<sub>2</sub>), 7.63 (d, 2H, J = 8.3, C<sub>6</sub>H<sub>4</sub>-N<sub>2</sub>), 7.65 (d, 2H, J = 8.3, C<sub>6</sub>H<sub>4</sub>-N<sub>2</sub>), 7.85 (d, 2H, C<sub>6</sub>H<sub>3</sub>). <sup>13</sup>C NMR (DMSO-*d*<sub>6</sub>) (ppm) δ: 34.78 (CH<sub>3</sub>-N), 57.10 (CH<sub>2</sub>), 114.39, 117.76, 118.63, 118.80 (3), 124.33, 126.40 (2), 127.84, 128.56 (3), 128.92 (3), 129.02 (3), 129.31 (2), 129.60 (2), 131.13, 131.94, 142.99, 169.73 (2); MS (*m/z*): 613.06 (M<sup>+</sup>, 11.67%), 553.70 (40.68%), 490.10 (59.29%), 404.81 (59.07%), 245.20 (56.46%), 61.64 (100%, base peak); Anal. Calcd for: C<sub>30</sub>H<sub>21</sub>ClN<sub>6</sub>O<sub>3</sub>S<sub>2</sub> (613.11): C, 58.77; H, 3.45; N, 13.71; S, 10.46. Found: C, 58.70; H, 3.40; N, 13.70; S, 10.40.

4.1.3.3. *2-Chloro-N-([4-{(4-[7-chloro-1-methyl-2-oxo-2,3-dihydro-1H-benzo[e][1,4]diazepin-5-yl]phenyl)-diazenyl]phenyl)sulfonyl}benzimidoyl-isothiocyanate (7c)*. Orange crystals; m.p. 255–157 °C; yield 86%; IR (KBr,  $\text{cm}^{-1}$ ): 2063 (N=C=S), 1693 (C=O), 1597 (N=N), 1152 ( $\text{SO}_2$ );  $^1\text{H}$  NMR ( $\text{DMSO-}d_6$ )  $\delta$ : 3.34 (s, 3H, N- $\text{CH}_3$ ), 4.01 (d, 1H,  $J = 10.8$ , CH methylene), 4.57 (d, 1H,  $J = 10.8$ , CH methylene), 7.27 (s, 1H,  $\text{C}_6\text{H}_3$ ), 7.53, 7.57 (dd, 4H,  $J = 7.6$ ,  $\text{C}_6\text{H}_4\text{-SO}_2$ ), 7.62, 7.65 (dd, 4H,  $J = 8.3$ ,  $\text{C}_6\text{H}_4\text{-N}_2$ ), 7.82–7.84 (dd, 2H,  $\text{C}_6\text{H}_3$ ).  $^{13}\text{C}$  NMR ( $\text{DMSO-}d_6$ ) (ppm)  $\delta$ : 35.02 ( $\text{CH}_3\text{-N}$ ), 52.16 ( $\text{CH}_2$ ), 95.75, 95.88, 120.00, 124.80 (2), 127.98 (2), 128.94 (2), 129.21, 132.48 (2), 133.71 (2), 136.73, 142.78 (2), 144.80 (NCS), 147.98 (2), 148.94, 157.93, 162.78, 166.73 (2CN), 168.61, 170.90, 179.78 (C=O); MS ( $m/z$ ): 646.65 ( $\text{M}^+$ , 14.71%), 636.71 (43.17%), 583.15 (50.54%), 427.33 (59.02%), 249.83 (68.63%), 189.67 (100%, base peak); Anal. Calcd for:  $\text{C}_{30}\text{H}_{20}\text{Cl}_2\text{N}_6\text{O}_3\text{S}_2$  (647.55): C, 55.56; H, 3.11; N, 12.98; S, 9.90. Found: C, 55.50; H, 3.10; N, 12.90; S, 9.90.

#### 4.2. Docking studies

In the present work, all the target compounds were subjected to docking study to explore their binding mode towards VEGFR-2 enzyme. All modeling experiments were performed using molsoft program, which provides a unique set of tools for the modeling of protein/ligand interactions. It predicts how small flexible molecule such as substrates or drug candidates bind to a protein of known 3D structure represented by grid interaction potentials ([http://www.molsoft.com/icm\\_pro.html](http://www.molsoft.com/icm_pro.html)). Each experiment used the biological target VEGFR-2 downloaded from the Brookhaven Protein Databank (<http://www.rcsb.org/pdb/explore/explore.do?structureId=1YWN>). In order to qualify the docking results in terms of accuracy of the predicted binding conformations in comparison with the experimental procedure, the reported VEGFR-2 inhibitor drug sorafenib was used as reference ligand.

#### 4.3. In vitro cytotoxic activity

Cancer cells from different cancer cell lines hepatocellular carcinoma (HepG2), breast cancer (MCF-7) and colorectal carcinoma (HCT-116), were purchased from American type Cell Culture collection (ATCC, Manassas, USA) and grown on the appropriate growth medium Roswell Park Memorial Institute medium (RPMI 1640) supplemented with 100 mg/mL of streptomycin, 100 units/mL of penicillin and 10% of heat-inactivated fetal bovine serum in a humidified, 5% (v/v)  $\text{CO}_2$  atmosphere at 37 °C Cytotoxicity assay by 3-[4,5-dimethylthiazole-2-yl]-2,5-diphenyltetrazolium bromide (MTT).

Exponentially growing cells from different cancer cell lines were trypsinized, counted and seeded at the appropriate densities (2000–1000 cells/0.33  $\text{cm}^2$  well) into 96-well microtiter plates. Cells then were incubated in a humidified atmosphere at 37°C for 24 h. Then, cells were exposed to different concentrations of compounds (0.1, 10, 100 and 1000  $\mu\text{M}$ ) for 72 h. Then the viability of treated cells was determined using MTT technique as follow. Cells were incubated with 200  $\mu\text{l}$  of 5% MTT solution/well (Sigma Aldrich, MO) and were allowed to metabolize the dye into colored-insoluble formazan crystals for 2 h. The remaining MTT solution were discarded from the wells and the formazan crystals were dissolved in 200  $\mu\text{l}$ /well acidified isopropanol for 30 min, covered with aluminum foil and with continuous shaking using a MaxQ 2000 plate shaker (Thermo Fisher Scientific Inc, MI) at room temperature. The colorimetric assay was measured and recorded at absorbance of 570 nm using a Stat FaxR 4200 plate reader (Awareness Technology, Inc., FL). The cell viability were expressed as percentage of control and the concentration that induces 50% of maximum inhibition of cell proliferation ( $\text{IC}_{50}$ ) were determined using Graph Pad Prism version 5 software (Graph Pad software Inc, CA) [49,72–74].

#### 4.4. In vitro VEGFR-2 kinase assay

The kinase activity of VEGFR-2 was measured by use of an anti-phosphotyrosine antibody with the Alpha Screen system (PerkinElmer, USA) according to manufacturer's instructions [49,72,74]. Enzyme reactions were performed in 50 mM Tris-HCl pH 7.5, 5 mM  $\text{MnCl}_2$ , 5 mM  $\text{MgCl}_2$ , 0.01% Tween-20 and 2 mM DTT, containing 10  $\mu\text{M}$  ATP, 0.1  $\mu\text{g}/\text{mL}$  biotinylated poly-GluTyr (4:1) and 0.1 nM of VEGFR-2 (Millipore, UK). Prior to catalytic initiation with ATP, the tested compounds at final concentrations ranging from 0 to 300  $\mu\text{g}/\text{mL}$  and enzyme were incubated for 5 min at room temperature. The reactions were quenched by the addition of 25  $\mu\text{l}$  of 100 mM EDTA, 10  $\mu\text{g}/\text{mL}$  Alpha Screen streptavidin donor beads and 10  $\mu\text{g}/\text{mL}$  acceptor beads in 62.5 mM HEPES pH 7.4, 250 mM NaCl, and 0.1% BSA. Plate was incubated in the dark overnight and then read by ELISA Reader (PerkinElmer, USA). Wells containing the substrate and the enzyme without compounds were used as reaction control. Wells containing biotinylated poly-GluTyr (4:1) and enzyme without ATP were used as basal control. Percent inhibition was calculated by the comparison of compounds treated to control incubations. The concentration of the test compound causing 50% inhibition ( $\text{IC}_{50}$ ) was calculated from the concentration–inhibition response curve (triplicate determinations) and the data were compared with Sorafenib (Sigma-Aldrich, USA) as standard VEGFR-2 inhibitor.

#### Declaration of Competing Interest

The authors declare that they have no known competing financial interests or personal relationships that could have appeared to influence the work reported in this paper.

#### Acknowledgments

The authors extend their appreciation and thanking to Dr. Fatma M. I. A. Shoman, MD in Clinical Pathology, Blood bank specialist, Blood bank directorate manager, Ministry of Health, Cairo, Egypt for helping in the pharmacological part.

#### Appendix A. Supplementary material

Supplementary data to this article can be found online at <https://doi.org/10.1016/j.bioorg.2020.104350>.

#### References

- [1] R. Manchanayake, Integrating Green and Sustainable Chemistry Principles into Education, 2019, pp. 117–139. <https://doi.org/10.1016/B978-0-12-817418-0.00005-X>.
- [2] I.H. El Azab, N.A.A. Elkanzi, An efficient synthetic approach towards Benzo[b]pyrro[2,3-*e*][1,4]diazepines, and their cytotoxic activity, *Molecules* 25 (9) (2020) 2051–2064, <https://doi.org/10.3390/molecules25092051>.
- [3] S. Verma, S. Kumar, S. Kumar, Design, synthesis, computational and biological evaluation of new benzodiazepines as CNS agents, *Arab. J. Chem.* 13 (2020) 863–874.
- [4] E. Sigel, M. Ernst, The benzodiazepine binding sites of GABAA receptors, *Trends Pharmacol. Sci.* 39 (2018) 659–671.
- [5] A.F. Gomez, A.L. Barthel, S.G. Hofmann, Comparing the efficacy of benzodiazepines and serotonergic anti-depressants for adults with generalized anxiety disorder: a meta-analytic review, *Expert Opin. Pharmacother.* 19 (2018) 883–894.
- [6] S. Gustafsson, V. Lindström, M. Ingelsson, M. Hammarlund-Udenaes, S. Syvänen, Intact blood-brain barrier transport of small molecular drugs in animal models of amyloid beta and alpha-synuclein pathology, *Neuropharmacology* 128 (2018) 482–491.
- [7] L.P. Tardibono, M.J. Miller, Synthesis and anticancer activity of new hydroxamic acid containing 1,4-benzodiazepines, *Org. Lett.* 11 (7) (2009) 1575–1578.
- [8] S. Chadha, S. Paul, K.K. Kapoor, Synthesis and biological screening of 4-(5-alkyl-2-isoxazolin-3-yl)-2-aryl-2,3-dihydro-1H-1,5-benzodiazepines, *J. Chem. Pharm. Res.* 3 (2011) 331–340.
- [9] A. Sachdeva, M. Choudhary, M. Chandra, Alcohol withdrawal syndrome: benzodiazepines and beyond, *J. Clin. Diagn. Res.* 9 (2015) VE01–VE07.

- [10] S. Kumaraswamy, C. Chien-Shu, C. Chi-Fen, P. Srinivas, M. Khagga, W. Chi-Rei, C. Ta-Hsien, Synthesis, anticonvulsant, sedative and anxiolytic activities of novel annulated pyrrolo[1,4]benzodiazepines, *Int. J. Mol. Sci.* 15 (2014) 16500–16510.
- [11] M. Soyka, Treatment of benzodiazepine dependence, *N. Engl. J. Med.* 376 (2017) 1147–1157.
- [12] M. Manconi, R. Ferri, S. Miano, M. Maestri, V. Bottasini, M. Zucconi, L. Ferini-Strambi, Sleep architecture in insomniacs with severe benzodiazepine abuse, *J. Clin. Neurophysiol.* 128 (2017) 875–881.
- [13] J. Guina, B. Merrill, Benzodiazepines I: upping the care on downers: the evidence of risks, benefits and alternatives, *J. Clin. Med.* 7 (2018) 1–22.
- [14] A. Shafie, M. Mohammadi-Khanaposhtani, M. Asadi, N. Rahimi, P.R. Ranjbar, J. B. Ghasemi, B. Larjani, M. Mahdavi, H. Shafaroodi, A.R. Dehpour, Novel fused 1,2,3-triazolo-benzodiazepine derivatives as potent anticonvulsant agents: design, synthesis, in vivo, and in silico evaluations, *Mol Divers* 24 (1) (2020) 179–189.
- [15] V.I. Pavlovsky, O.V. Tsybalyuk, V.S. Martynyuk, T.A. Kabanova, E. A. Semishyna, E.I. Khalimova, S.A. Andronati, Analgesic effects of 3-substituted derivatives of 1,4-benzodiazepines and their possible mechanisms, *Neurophysiology* 45 (2013) 427–432.
- [16] A.A.S. Bader, A.H. Omar, M.H. El-Odemi, Anti-inflammatory effects of diazepam on different models of inflammation: roles of peripheral benzodiazepine receptors and genes for corticosterone, nitric oxide and cytokines biosynthesis, *J. Clin. Epigenet.* 3 (2017) 1–8.
- [17] L. Jing-Jing, W. Xin-Ying, C. Jing-Lou, C. Guan-Rong, X. Jun, G. Ye, S. Hong-Ping, Antiplatelet drug ticagrelor delays gastric ulcer healing in rats, *Exp. Ther. Med.* 14 (2017) 3774–3779.
- [18] A. Włodarczyk, J. Szarmach, W.J. Cubala, M.S. Wiglusz, Benzodiazepines in combination with antipsychotic drugs for schizophrenia: GABA-ergic targeted therapy, *Psychiatr Danub.* 29 (2017) 345–348.
- [19] A.A. Mahmoud, W.M. El-Sayed, The anti-proliferative activity of anisocadione: a new guaiane sesquiterpene from anisocadioid lanatum, *Anti-Cancer Agents Med. Chem.* 19 (2019) 1114–1119.
- [20] Q. Zhang, Q. Shen, L. Gao, L. Tong, J. Li, Y. Chen, W. Lu, Pyrazolo[4,3-b]pyrimido [4,5-e] [1,4]diazepine derivatives as new multi-targeted inhibitors of Aurora A/B and KDR, *Eur. J. Med. Chem.* 5 (2018) 428–441.
- [21] C. Kurokawa, H. Geekiyanage, C. Allen, I. Iankov, M. Schroeder, B. Carlson, K. Bakken, J. Sarkaria, J.A. Ecsedy, A. D'Assoro, B. Friday, E. Galanis, Alisertib demonstrates significant antitumor activity in bevacizumab resistant, patient derived orthotopic models of glioblastoma, *J. Neurooncol.* 131 (1) (2017) 41–48.
- [22] T.B. Sells, R. Chau, J.A. Ecsedy, R.E. Gershman, K. Hoar, J. Huck, D.A. Janowick, V. J. Kadambi, P.J. Leroy, M. Stirling, MLN8054 and alisertib (MLN8237): discovery of selective oral aurora a inhibitors, *ACS Med. Chem. Lett.* 6 (2015) 630.
- [23] D.-H. Kim, J.-T. Lee, I.-K. Lee, J.-H. Ha, Comparative anticancer effects of flavonoids and diazepam in cultured cancer cells, *Biol. Pharm. Bull.* 31 (2) (2008) 255–259.
- [24] I. Balderas-Renteria, P. González-Barranco, A. García, B.K. Banik, G. Rivera, Anticancer drug design using scaffolds of B-lactams, sulfonamides, quinoline, quinoxaline and natural products, *Drugs Adv. Clinical Trials. CMC* 19 (2012) 4377–4398.
- [25] M.S.A. El-Gaby, Z.H. Ismail, S.M. Abdel-Gawad, H.M. Aly, M.M. Ghorab, Synthesis of thiazolidine and thioephene derivatives for evaluation as anticancer agents, *Phosphorus Sulfur Silicon Related Elements* 184 (10) (2009) 2645–2654.
- [26] R.M. Okasha, M. Elsehli, S. Ihmaid, S.S. Althagfan, M.S.A. El-Gaby, H.E.A. Ahmed, T.H. Afifi, First example of Azo-Sulfa conjugated chromene moieties: synthesis, characterization, antimicrobial assessment, docking simulation as potent class I histone deacetylase inhibitors and antitumor agents, *Bioorg. Chem.* 92 (2019) 103262, <https://doi.org/10.1016/j.bioorg.2019.103262>.
- [27] M.M. Ghorab, M.S. Alsaid, M.S.A. El-Gaby, N.A. Safwat, M.M. Elasser, A. M. Soliman, Biological evaluation of some new N-(2,6-dimethoxyimidazole) thiourea benzene sulfonamide derivatives as potential antimicrobial and anticancer agents, *Eur. J. Med. Chem.* 124 (2016) 299–310.
- [28] M.S.A. El-Gaby, M.M. Ghorab, Z.H. Ismail, S.M. Abdel-Gawad, H.M. Aly, Synthesis, structural characterization and anticancer evaluation of pyrazole derivatives, *Med. Chem. Res.* 27 (1) (2018) 72–79.
- [29] M. Ghorab, F. Ragab, H. Heiba, M. El-Gazzar, M. El-Gazzar, Synthesis, in vitro anticancer screening and radiosensitizing evaluation of some new 4-[3-(substituted)thiourea]-N-(quinoxalin-2-yl)-benzenesulfonamide derivatives, *Acta Pharmaceutica* 61 (2011) 415–425.
- [30] M.I. Shahin, D.A.A. El Ella, N.S. Ismail, K.A. Abouzid, Design, synthesis and biological evaluation of type-II VEGFR-2 inhibitors based on quinoxaline scaffold, *Bioorg. Chem.* 56 (2014) 16–26.
- [31] A.M.S. El Newahie, N.S.M. Ismail, D.A.A. El Ella, K.A.M. Abouzid, Quinoxaline-based scaffolds targeting tyrosine kinases and their potential anticancer activity, *Arch. Pharm. Chem. Life Sci.* 349 (2016) 309–326.
- [32] S. Madhusudan, T.S. Ganesan, Tyrosine kinase inhibitors in cancer therapy, *Clin. Biochem.* 37 (2004) 618–635.
- [33] A.J. Hoefnagel, H. Van Koningsveld, F. Van Meurs, J.A. Peters, A. Sinnema, H. Van Bekkum, Reactions of hydroxyglycines. New synthetic routes to 4-phenylquinazoline derivatives, *Tetrahedron* 49 (1993) 6899–6912.
- [34] X. Zhong, H.-L. Wei, W.-S. Liu, D.-Q. Wang, X. Wang, The crystal structures of copper(II), manganese(II), and nickel(II) complexes of a (Z)-2-hydroxy-N'-(2-oxindolin-3-ylidene) benzohydrazide—potential antitumor agents, *Bioorg. Med. Chem. Lett.* 17 (13) (2007) 3774–3777.
- [35] J. Mirzaei, et al., Convenient syntheses of 5-[(2-methyl-5-nitro-1H-imidazol-1-yl) methyl]-1, 3, 4-oxadiazole-2 (3H) thione and N-substituted 2-amino-5-[(2-methyl-5-nitro-1H-imidazol-1-yl) methyl]-1, 3, 4-thiadiazoles, *J. Heterocyclic Chem.* 45 (3) (2008) 921–925.
- [36] P.M. Hoff, K.K. Machado, Role of angiogenesis in the pathogenesis of cancer, *Cancer Treat. Rev.* 38 (7) (2012) 825–833.
- [37] Z.K. Otrrock, J.A. Makarem, A.I. Shamseddine, Vascular endothelial growth factor family of ligands and receptors, *Blood Cells Mol. Dis.* 38 (3) (2007) 258–268.
- [38] E.S. Gershtein, E.A. Dubova, A.I. Shchegolev, N.E. Kushkinkii, Vascular endothelial growth factor and its type 2 receptor in hepatocellular carcinoma, *Bull. Exp. Biol. Med.* 149 (6) (2010) 749–752.
- [39] N.R. Smith, D. Baker, N.H. James, K. Ratcliffe, M. Jenkins, S.E. Ashton, G. Sproat, R. Swann, N. Gray, A. Ryan, J.M. Jurgensmeier, C. Womack, Vascular endothelial growth factor receptors VEGFR-2 and VEGFR-3 are localized primarily to the vasculature in human primary solid cancers, *Clin. Cancer Res.* 16 (14) (2010) 3548–3561.
- [40] H. Wei, et al., Design, synthesis and biological evaluation of novel 4-anilinoquinazoline derivatives as hypoxia-selective EGFR and VEGFR-2 dual inhibitors, *Eur. J. Med. Chem.* 181 (2019) 111552.
- [41] M.A. Abdullaziz, H.T. Abdel-Mohsen, A.M. El Kerdawy, F.A.F. Ragab, M.M. Ali, S. M. Abu-bakr, A.S. Girgis, H.I. El Diwani, Design, synthesis, molecular docking and cytotoxic evaluation of novel 2-furybenzimidazoles as VEGFR-2 inhibitors, *Eur. J. Med. Chem.* 136 (2017) 315–329.
- [42] L. Huang, Z. Huang, Z. Bai, R. Xie, L. Sun, K. Lin, Development and strategies of VEGFR-2/KDR inhibitors, *Future Med. Chem.* 4 (14) (2012) 1839–1852.
- [43] J.E. Frampton, Lenvatinib: a review in refractory thyroid cancer, *Target. Oncol.* 11 (2016) 115–122.
- [44] S. Takahashi, Vascular endothelial growth factor (VEGF), VEGF receptors and their inhibitors for antiangiogenic tumor therapy, *Biol. Pharm. Bull.* 34 (12) (2011) 1785–1788.
- [45] J. Kankanala, et al., A combinatorial in silico and cellular approach to identify a new class of compounds that target VEGFR2 receptor tyrosine kinase activity and angiogenesis, *British J. Pharmacol.* 166 (2) (2012) 737–748.
- [46] P. Wu, T.E. Nielsen, M.H. Clausen, FDA-approved small-molecule kinase inhibitors, *Trends Pharmacol. Sci.* 36 (7) (2015) 422–439.
- [47] S. Wilhelm, C. Carter, M. Lynch, T. Lowinger, J. Dumas, R.A. Smith, B. Schwartz, R. Simantov, S. Kelley, Discovery and development of sorafenib: a multikinase inhibitor for treating cancer, *Nat. Rev. Drug Discov.* 5 (10) (2006) 835–844.
- [48] A. Pircher, et al., Biomarkers in tumor angiogenesis and anti-angiogenic therapy, *Int. J. Mole. Sci.* 12 (10) (2011) 7077–7099.
- [49] K. El-Adl, A.-G. El-Helby, H. Sakr, I.H. Eissa, S.S.A. El-Hddad, F. M.I.A. Shoman, Design, synthesis, molecular docking and anticancer evaluations of 5-benzylidene-nethiazolidine-2,4-dione derivatives targeting VEGFR-2 enzyme, *Bioorg. Chem.* 102 (2020) 104059, <https://doi.org/10.1016/j.bioorg.2020.104059>.
- [50] A.-G. El-Helby, H. Sakr, I.H. Eissa, A.A. Al-Karmalawy, K. El-Adl, Benzoxazole/benzothiazole-derived VEGFR-2 inhibitors: design, synthesis, molecular docking, and anticancer evaluations, *Arch. Pharm. Chem. Life Sci.* 352 (12) (2019) 1900178, <https://doi.org/10.1002/ardp.v352.1210.1002/ardp.201900178>.
- [51] H.A. Mahdy, et al., Design, synthesis, molecular modeling, in vivo studies and anticancer evaluation of quinazolin-4 (3H)-one derivatives as potential VEGFR-2 inhibitors and apoptosis inducers, *Bioorg. Chem.* 94 (2020) 103422.
- [52] A.-G. El-Helby, H. Sakr, I.H. Eissa, H. Abulkhair, A.A. Al-Karmalawy, K. El-Adl, Design, synthesis, molecular docking, and anticancer activity of benzoxazole derivatives as VEGFR-2 inhibitors, *Arch. Pharm. Chem. Life Sci.* 352 (10) (2019) 1900113, <https://doi.org/10.1002/ardp.v352.1010.1002/ardp.201900113>.
- [53] A.-G.-A. El-Helby, H. Sakr, R.R.A. Ayyad, K. El-Adl, M.M. Ali, F. Khedr, Design, synthesis, in vitro anti-cancer activity, ADMET profile and molecular docking of novel triazolo [3, 4-a] phthalazine derivatives targeting VEGFR-2 enzyme, *Anti-Cancer Agents Med. Chem. (Form. Curr. Med. Chem.-Anti-Cancer Agents)* 18 (8) (2018) 1184–1196.
- [54] A.-G. El-Helby, R.R.A. Ayyad, H. Sakr, K. El-Adl, M.M. Ali, F. Khedr, Design, synthesis, molecular docking, and anticancer activity of phthalazine derivatives as VEGFR-2 inhibitors: phthalazine derivatives as VEGFR-2 inhibitors, *Arch. Pharm. Chem. Life Sci.* 350 (12) (2017) 1700240, <https://doi.org/10.1002/ardp.201700240>.
- [55] M.M. Khowdiary, N.S. Mostafa, Synthesis of sulfadimethoxine based surfactants and their evaluation as antitumor agents, *J. Cancer Res. Ther.* 12 (1) (2016) 137–141, <https://doi.org/10.4103/0973-1482.172109>.
- [56] N.M. Saleh, M.G. El-Gazzar, H.M. Aly, R.A. Othman, Novel anticancer fused pyrazole derivatives as EGFR and VEGFR-2 dual TK inhibitors, *Front. Chem.* 7 (2020) 917, <https://doi.org/10.3389/fchem.2019.00917>.
- [57] Q.-Q. Xie, H.-Z. Xie, J.-X. Ren, L.-L. Li, S.-Y. Yang, Pharmacophore modeling studies of type I and type II kinase inhibitors of Tie2, *J. Mol. Graph. Model.* 27 (6) (2009) 751–758.
- [58] K. Lee, K.-W. Jeong, Y. Lee, J.Y. Song, M.S. Kim, G.S. Lee, Y. Kim, Pharmacophore modeling and virtual screening studies for new VEGFR-2 kinase inhibitors, *Eur. J. Med. Chem.* 45 (11) (2010) 5420–5427.
- [59] V.A. Machado, D. Peixoto, R. Costa, H.J.C. Froufe, R.C. Calheta, R.M.V. Abreu, I. C.F.R. Ferreira, R. Soares, M.-J. Queiroz, Synthesis, antiangiogenesis evaluation and molecular docking studies of 1-aryl-3-[(thieno[3,2-b]pyridin-7-ylthio)phenyl] ureas: discovery of a new substitution pattern for type II VEGFR-2 Tyr kinase inhibitors, *Bioorg. Med. Chem.* 23 (19) (2015) 6497–6509.
- [60] Z. Wang, et al., Dietary compound isoliquiritigenin inhibits breast cancer neoangiogenesis via VEGF/VEGFR-2 signaling pathway, *PLoS One* 8 (7) (2013).
- [61] J. Dietrich, C. Hulme, L.H. Hurley, The design, synthesis, and evaluation of 8 hybrid DFG-out allosteric kinase inhibitors: a structural analysis of the binding interactions of Gleevec®, Nexavar®, and BIRB-796, *Bioorg. Med. Chem.* 18 (15) (2010) 5738–5748.

- [62] M. Rashid, R. Mishra, A. Husain, B. Ahmad, Synthesis of some novel C3 substituted new diazo-[1,4]- benzodiazepine-2-one derivatives as potent anticonvulsants, *Chem. Sci. J.* 5 (2010) 1–9.
- [63] S. Sathish Kumar, H.P. Kavitha, S. Arulmurugan, B.R. Venkatraman, Review on synthesis of biologically active diazepam derivatives, *Mini-Rev. Org. Chem.* 9 (2012) 285, <https://doi.org/10.2174/1570193X11209030285>.
- [64] F.A. Carey, R.J. Sundberg, *Advanced Organic Chemistry, Part A: Structure and Mechanisms*, Chapter 9. Aromatic Substitution, 5th ed., 2007.
- [65] I. Nakatsuka, K. Kawahara, T. Kamada, F. Shono, A. Yoshitake, Synthesis of 7-chloro-1,3-dihydro-5-(2-fluorophenyl)-1-methyl-2H-1,4-benzodiazepin-2-one-5-<sup>14</sup>C (fludiazepam-1<sup>4</sup>C), *J. Label Compd. Radiopharm.* 13 (4) (1977) 453–459.
- [66] R.J. Ouellette, J.D. Rawn, in: *Organic Chemistry*, Elsevier, 2018, pp. 801–828, <https://doi.org/10.1016/B978-0-12-812838-1.50025-6>.
- [67] B.C. Ranu, R. Jana, Ionic liquid as catalyst and reaction medium – a simple, efficient and green procedure for knoevenagel condensation of aliphatic and aromatic carbonyl compounds using a task-specific basic ionic liquid, *Eur. J. Org. Chem.* 2006 (16) (2006) 3767–3770.
- [68] I. Elghamry, M. Abdelsalam, Expedient phosgene-free synthesis of symmetrical diarylureas from carbamates, *Arkivoc*, 2019, part vi, 83–92.
- [69] F.W. Askar, Y.A. Aldhalf, N.A. Jinzeel, et al., Synthesis and biological evaluation of new sulfonamide derivatives, *Int. J. Chem. Sc.* 15 (3) (2017) 173.
- [70] K.G. Bedane, G.S. Singh, Reactivity and diverse synthetic applications of acyl isothiocyanates, *ARKIVOC* 2015 (vi) 206–245.
- [71] S. El-Feky, et al., Design, synthesis and in vitro antitumor activity of novel phthalazin-1, 4-dione/chalcone hybrids and phthalazin-1, 4-dione/pyrazoline hybrids, *J. Chem. Pharmac. Res.* 7 (7) (2015) 1154–1166.
- [72] F.M. Freimoser, et al., The MTT [3-(4, 5-dimethylthiazol-2-yl)-2, 5-diphenyltetrazolium bromide] assay is a fast and reliable method for colorimetric determination of fungal cell densities, *Appl. Environ. Microbiol.* 65 (8) (1999) 3727–3729.
- [73] K. El-Adl, H. Sakr, M. Nasser, M. Alswah, F.M.A. Shoman, 5-(4-Methoxybenzylidene)thiazolidine-2,4-dione-derived VEGFR-2 inhibitors: design, synthesis, molecular docking, and anticancer evaluations, *Arch Pharm.* (2020), <https://doi.org/10.1002/ardp.202000079>.
- [74] K. El-Adl, A.-G.A. El-Helby, H. Sakr, S.S.A. El-Hddad, Design, synthesis, molecular docking, and anticancer evaluations of 1-benzylquinazoline-2,4(1H,3H)-dione bearing different moieties as VEGFR-2 inhibitors, *Arch Pharm.* (2020), <https://doi.org/10.1002/ardp.202000068>.